Journal of Hydrology: Regional Studies 58 (2025) 102253

Contents lists available at ScienceDirect

Journal of Hydrology: Regional Studies

journal homepage: www.elsevier.com/locate/ejrh

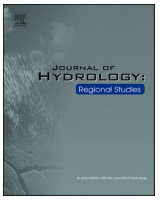

Widespread pH increase and geochemical trends in fifty boreal lakes: Evidence, prediction and plausible attribution to climate and permafrost thaw impacts across northeastern Alberta

J.J. Gibson [a,b,*], A. Jaggi [c], F.J. Castrillon-Munoz [c,1]

[a] InnoTech Alberta, 3-4476 Markham Street, Victoria, BC V8Z 7×8, Canada
[b] University of Victoria, Geography, Victoria, BC V8W 3R4, Canada
[c] InnoTech Alberta, 3608 - 33 St NW, Calgary, Alberta T2L 2A6, Canada

ARTICLE INFO

Keywords:
Boreal lakes
Permafrost
pH
Major ions
Water isotopes
Carbon cycle

ABSTRACT

Study region: This study focuses on 50 boreal lakes and catchments situated in northeastern Alberta, Canada between 55.68°N – 59.72°N and 110.02°W – 115.46°W.
Study focus: Evidence for trends in chemical composition of lakes, including pH increases are provided using Mann-Kendall statistics, geochemical modelling, $\delta^{18}O$, $\delta^{2}H$, and $\delta^{13}C$, which are compared to trend statistics for climate, water balance, and groundwater indicators.
New hydrological insights for the region: Groundwater contributions are generally found to be increasing with water yield and carbon inputs as sites advance along the thaw trajectory. The exception to this is shield lakes which continue to be surface water dominant. Statistical analyses suggest widespread trends, both significant and non-significant, in geochemical parameters across the lake network including pH increases in 46 of 50 lakes. In shale-dominated plateau areas, pH trends are adequately described by changes in HCO_3^-, attributed mainly to carbon input associated with permafrost thaw. For these lakes, prediction improves little if other variables are considered, whereas for post thaw areas, prediction of pH trends improves if water yield trends are also considered. In sub-regions with appreciable carbonate, pH trend prediction improves significantly if values of $\delta^{13}C_{DIC}$ and Dissolved Inorganic Carbon (DIC) are also considered. We postulate that recent pH trends across the region may only be temporary and that lake acidification may yet occur once permafrost thaw and related carbon imports diminish.

1. Introduction

Detectable long-term changes in water quality and water quantity have occurred in lakes and rivers across the Alberta Oil Sands region over the past few decades, as revealed through combined analysis of contemporary environmental monitoring datasets (e.g., Alexander and Chambers, 2016) and paleolimnological records (e.g., Curtis et al., 2010; Summers et al., 2016; Cooke et al., 2017; Zabel et al., 2021). While clear attribution of detectable changes to concurrent development pressures such as oil sands airborne emissions and/or site development has been argued by several previous investigators (e.g., Schindler, 2014; Kelly et al., 2009,2010; Kurek et al., 2013), these assertions remain a topic of some controversy owing to incomplete understanding of water and geochemical processes

* Correspondence to: 3-4476 Markham Street, Victoria, BC V8Z 7× 8, Canada
E-mail address: jjgibson@uvic.ca (J.J. Gibson).
[1] Current address: Summit Earth, 430–7220 Fisher St. SE Calgary Alberta T2H 2H8 Canada.

https://doi.org/10.1016/j.ejrh.2025.102253
Received 26 September 2024; Received in revised form 12 February 2025; Accepted 13 February 2025
Available online 26 February 2025
2214-5818/Crown Copyright © 2025 Published by Elsevier B.V. This is an open access article under the CC BY license (http://creativecommons.org/licenses/by/4.0/).

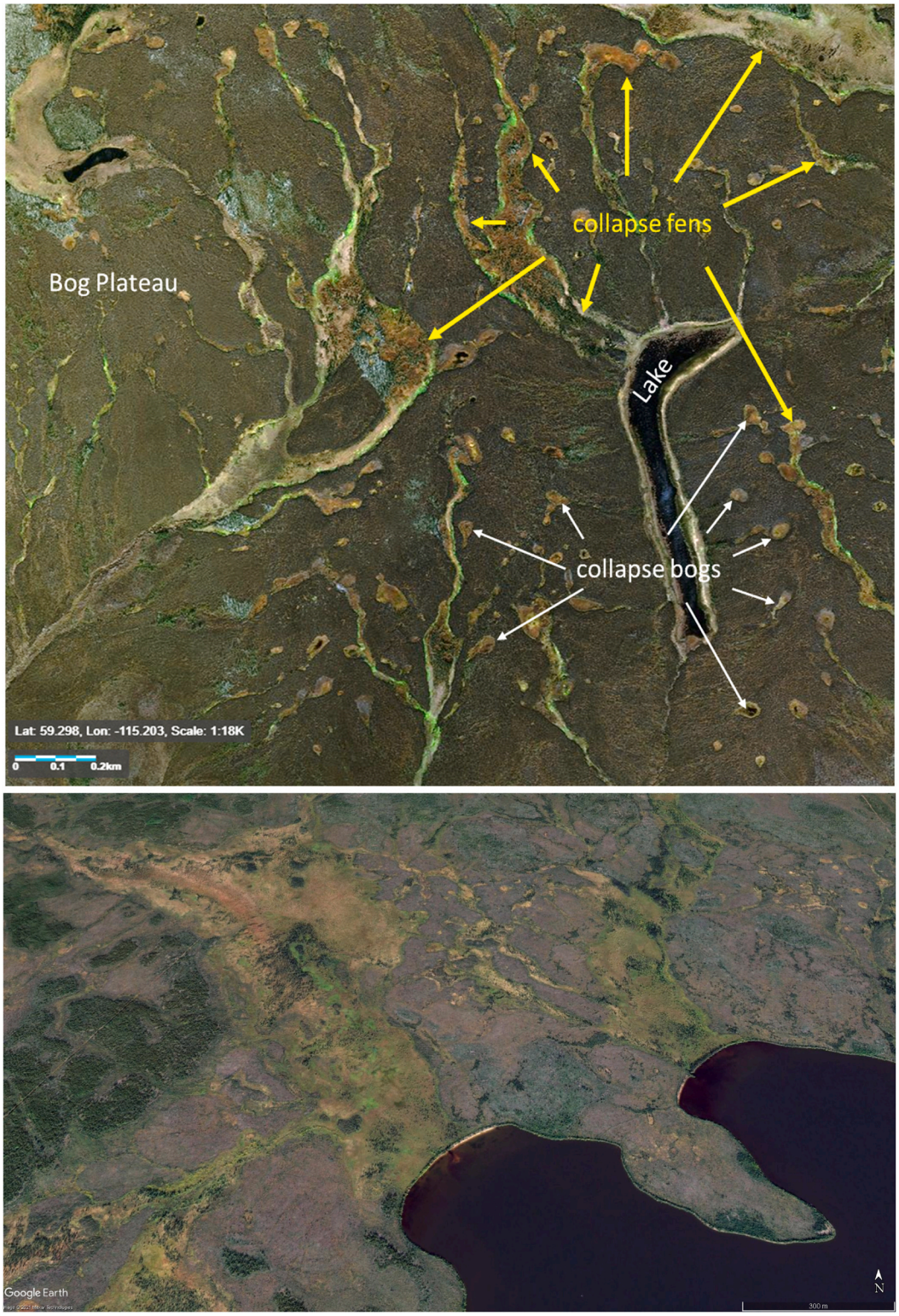

Fig. 1. Google Earth images showing selected permafrost thaw features: (a)(top panel) vertical satellite image of bog plateau in the Caribou Mountains with collapse features attributed to permafrost thaw; and (b) (bottom panel) oblique satellite image of shoreline collapse fens adjacent to RAMP Lake BM1 evident as highly productive green/tan collapse scars. Arrows identify collapse bogs and fens.

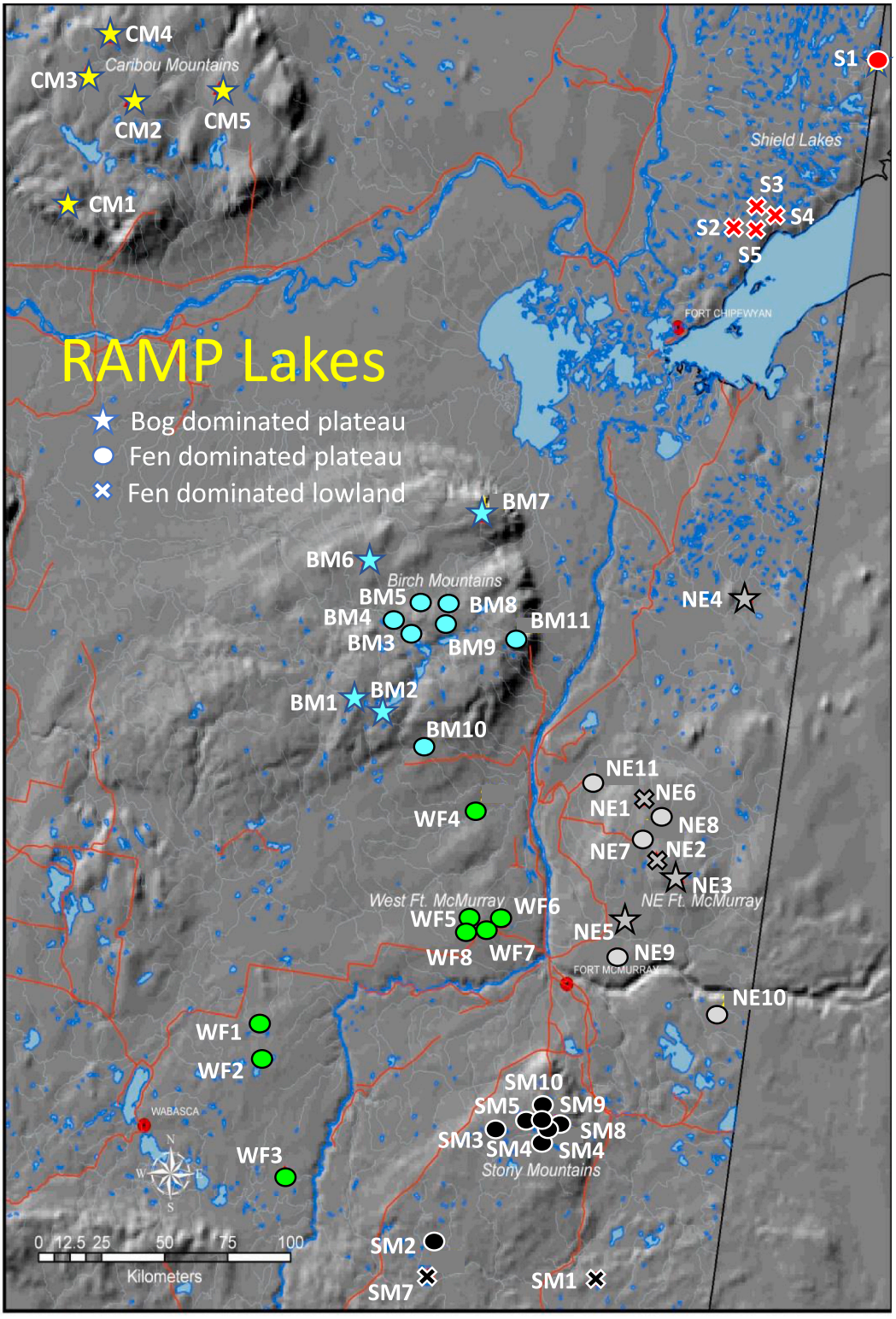

Fig. 2. Map showing location of the RAMP lakes colour coded by subregion. Star symbols denote bog dominated plateau lakes, circles denote fen dominated plateau lakes, and crosses denote fen dominated lowland lakes. Vertical exaggeration highlights contrast in elevation between regional upland plateaus and interceding lowlands.

across the region, and in many cases, due to inability to resolve between natural and anthropogenic constituents (Culp et al., 2021). Despite long-standing perspectives on climate-landscape evolution established from peatland studies across the region (Vitt et al., 1994; Beilman et al., 2000), and evidence for ongoing hydroclimatic changes (e.g., Bonsal et al., 2019; Eum et al., 2017; Peters et al., 2022), relatively little attention has been paid in past water quality assessments to the larger backdrop of regional climate change. Impacts on water quantity and quality may be influenced by observed increases in air temperatures, modification of precipitation patterns and snowcover, shifts in the timing of runoff and recharge, reduction in ice-cover duration, and permafrost thaw (Jiang et al., 2017; Gratton and Béllanger, 2018; Gibson et al., 2015, 2019a, 2020; Zolkos and Tank, 2020; Spence et al., 2020). Bog plateau collapse due to permafrost thaw has visibly scarred the landscape across regional uplands or plateaus such as the Birch and Caribou Mountains (e.g., Fig. 1), and permafrost thaw appears to remain influential in lowland peat complexes such as the McClelland Fen that host sporadic or isolated permafrost (see Vitt et al., 2022). Elsewhere across the largely undeveloped circumboreal and circumpolar regions, such changes have been convincingly linked to significant alteration in the water, carbon and biogeochemical cycles of lakes and rivers (e.g., Holmes et al., 2008, 2013; in't Zandt et al., 2020; Walvoord and Streigl, 2021; Webb et al., 2022; Schuur et al., 2018, 2022; Wu et al., 2023). Based on these precedents, and many similarities between what is occurring in the oil sands region and in similar settings across the northern hemisphere, there is an urgent need for climate and development to be considered together within the context of ongoing assessments and impact attribution studies in the oil sands region.

The main objective of this investigation has been to describe systematic geochemical and isotopic changes that have occurred in the RAMP lakes in northeastern Alberta over the past two decades, notably to better understand processes driving water yield increases in the watersheds (Gibson et al., 2015, 2019a) as well as the underlying causes of monotonic pH increases detected in 46 of 50 lakes (Castrillon et al., 2022). In doing so, we have been compelled to reconsider our initial working hypothesis that the lakes were likely to acidify due to oil sands emissions (Gibson et al., 2010a, 2010b), and to consider a broader alternative hypothesis that current geochemical changes may plausibly be influenced or dominated by climate change effects. In support, we present and evaluate both direct and indirect site-specific evidence of concurrent climatic and hydrologic changes in the lake-watershed systems including surface and groundwater inputs estimated by isotopic methods, and draw on previous studies that mapped land cover, permafrost extent, and permafrost collapse scar extent in the watersheds. Together, these studies indicate systematic causal links between climate changes, water balance changes, and the observed geochemical changes in the lakes. While additional studies will be required to verify our supposition, we offer a testable hypothesis that landscape water yields will decrease progressively until permafrost is completely thawed, so that temporary increases in pH will eventually subside and regional lake acidification may proceed under drier hydrologic and climatic conditions.

1.1. Study sites and site selection

Alberta's Oil Sands deposits are among the largest bitumen reserves in the world, containing an estimated 170 billion barrels or roughly 13 % of proven petroleum reserves globally (Gosselin et al., 2010; Gibson and Peters, 2022). Prior to establishment of the current provincial-federal Oil Sands Monitoring (OSM) program in 2012, the Regional Aquatics Monitoring Program (RAMP) was established in 1997 as a joint industry-government monitoring program aimed at assessing the health of rivers and lakes across the region. Water quality monitoring within RAMP has largely centred on assessment of the risk of acidification of soils, wetlands and lakes due to current and projected emissions from mining, in-situ production and upgrading of bitumen (http://www.ramp-alberta.org/RAMP.aspx). In addition to rivers and wetlands, a network of 50 lakes was chosen for annual monitoring from an initial survey of 460 lakes (WRS, 2006). Detailed land cover mapping was carried out in 2008 using 1:18:000 scale black and white air photos, differentiating 40 land cover classes (D. Vitt, pers. Comm.) applying methodology consistent with Halsey et al. (2003). A land cover summary including PCA analysis of hydrologic drivers was provided by Gibson et al. (2015). Watershed and lake characteristics and hydrologic information was described by Gibson et al. (2019a) and data were published in Gibson et al. (2020).

The lakes are divided into six geographic sub-regions and span a range in latitude between 55.68°N and 59.72°N and longitude between 110.02°W and 115.46°W (Fig. 2). Collectively, the lakes and their watersheds are considered to be representative of the three main lake-watershed types in the region, i.e., bog-dominated permafrost-rich plateau (BDP), fen-dominated plateau (FDP), and fen-dominated lowlands (FDL), where fen-dominated sites are typically permafrost-poor. 40 of 50 lakes are situated within 200 km of the centre of regional oil sands operations (see Bennett et al., 2008) intended to serve as sentinel sites to gauge acid emission effects. The RAMP lakes include 10 lakes in the Stony Mountains (SM), 11 lakes in the Birch Mountains (BM), 8 lakes west of the city of Fort McMurray (WM) and 11 lakes northeast (NE) of the city of Fort McMurray (Fig. 2). Lake groups outside of the 200-km radius include 5 lakes situated on the Precambrian Shield to the west of Lake Athabasca (S) and 5 lakes situated in the Caribou Mountains (CM). Lakes range from small (3.4 ha) to large (4400 ha), with depths ranging from 1 to 30 m, although most lakes are shallow, i.e., 46 lakes are less than 4 m depth). Watersheds vary in size from 57 ha to 16,555 ha, with percentage lake area ranging from 1 % to 30 % (Gibson et al., 2015, 2019a, 2020).

The RAMP lakes are situated predominantly in headwater catchments across a range of latitude, morphometry and wetland-rich landscapes (Gibson et al., 2010a). The lakes in the Stony and Birch Mountains are situated on peat plateaus underlain by weathered shales of the Cretaceous Colorado Group that form a shallow, low-permeability barrier to vertical groundwater movement. Shield lakes are situated in areas underlain by crystalline Precambrian Shield bedrock covered by a shallow, discontinuous mantle of glacial till. In all other subregions, lakes are underlain by Quaternary tills, sandstones, siltstones, shales and carbonates of Cretaceous to Devonian age. Such areas typically have higher permeability than the peat plateaus which allows for greater potential interaction with groundwater. Buried erosional channels filled with Quaternary/Tertiary sediments are a common feature of the region, and similar to stream channels, may serve as conduits of inflow or outflow to nearby lakes (Gibson et al., 2019b).

1.2. Previous studies

Previous studies of lakes in the region have focused on water balance and geochemistry with the purpose of understanding and monitoring potential sensitivity to forest management practices (e.g., Prepas et al., 2001; Gibson et al., 2002; Devito et al., 2005, 2017; Smerdon et al., 2005), surface/groundwater interaction (Schmidt et al., 2010), and acidification due to deposition of sulfur and nitrogen compounds related to Alberta Oil Sands development (Gibson et al., 2010a, 2010b; Makar et al., 2018). Previous isotopic assessments have established that hydrology and geochemistry of lakes and watersheds may also be influenced by permafrost thaw, which serves to increase water yield from the watershed and buffers acidification (Gibson et al., 2015, Gibson et al., 2016, Gibson et al., 2019a; Castrillon-Munoz et al., 2022). A recent Mann-Kendall trend analysis has indicated widespread pH increase in lakes over the past two decades that may be occurring due to climatic shifts including permafrost thaw and bog/fen collapse (Gibson et al., 2019a), although the potential role of changes in groundwater/surface water interaction has yet to be evaluated. Groundwater recharge, surface water/groundwater interaction and permafrost thaw are expected to leave geochemical fingerprints on lake water similar to that noted for area rivers (Jasechko et al., 2012; Gibson et al., 2013; Birks et al., 2018, 2019) and may play a direct or indirect role in controlling the pH of runoff and/or lake water.

Given environmental concern for lake acidification related to oil sands activities, initial assessments of the RAMP lakes applied a steady-state water chemistry model similar to that of Henriksen et al. (2002) to predict critical loads of acidity. These early assessments utilized annual RAMP water chemistry data coupled with watershed runoff estimates approximated from a limited number of stream gauges in the region (e.g., WRS, 2006). Subsequent critical loads and exceedance assessments applied a similar framework but relied on site-specific stable-isotope-based estimates of runoff (Bennett et al., 2008), which were later updated based on longer, more reliable stable isotope and water chemistry records (Gibson et al., 2010a). This assessment was also informed by a multi-year field programs focused on representative watersheds in the Stony Mountains (SM8) and Muskeg Mountains (NE7), as described by Tattrie (2011) and Schmidt et al. (2010). Critical loads assessments were also carried out for contributing wetlands (Whitfield et al., 2010), which lay the foundation for a more comprehensive program of nitrogen amendment experiments to assess the fate of nitrogen deposited in representative terrain units (Berryman et al., 2016; Gibson et al., 2021). While the latter study was conducted at sites located outside of the RAMP lakes watersheds, they were located in terrain units typical of bog, fen and upland variations found in many of the RAMP watersheds.

More recent hydrology investigations in the RAMP watersheds have documented that permafrost thaw has a significant and apparently temporally variable effect on watershed runoff to lakes (Gibson et al., 2015, 2019a, 2020). The latest geochemical assessment of the RAMP lakes also revealed strong evidence that carbonate equilibria are actively being altered in the lakes (Castrillon et al., 2022), a process likely influenced by one or several factors such as permafrost thaw, surface/groundwater exchange, or CO_2 exchange due to longer open water season. In the case of permafrost thaw, carbon sources such as dissolved organic carbon (DOC) and dissolved inorganic carbon (DIC) are likely being mobilized and transported to lakes, as shown for thermokarst systems in northern Canada and Tibet (Wan et al., 2019a, 2019b, 2020). Similarly, thawing permafrost may alter fundamental interaction between lakes and groundwater due to deepening of the active layer, formation of taliks, or transition to seasonally frozen ground (Wan et al., 2019a). Paleohydrology studies in the oil sands region have also demonstrated an increase in temperature over the past century (Zabel et al., 2022) as well as a significant increase in productivity (eutrophication) in some lakes (Summers et al., 2016).

2. Methods

2.1. Water sampling

Water quality sampling was carried out by Alberta Environment staff adhering to the protocols outlined in Alberta Environment (2002), (2006) and RAMP (2005) (see also Hatfield Consultants Ltd. et al., 2016 for scope and history of the program). Sampling occurred in late summer or early fall (late August to early October) after thermal stratification had ended in most lakes, and during the subsequent weeks when the lakes are typically well mixed. Lakes were sampled by float plane or helicopter, as determined by size and logistics, and sampled near the lake centroid For float plane sampling events, column-integrated water samples from the euphotic zone (i.e., surface to Secchi depth) were collected by inserting weighted Tygon tubing outfitted with a one-way valve which was closed to withdraw the sample. This was repeated several times and samples were bulked together. Sampling within 1 m of the lake bottom was avoided. For smaller lakes sampled by helicopter, 1 L grab samples were collected at 0.5 m below surface. Water samples for geochemical analysis were stored at 4°C until returned for analysis.

Water samples for $\delta^{18}O$ and $\delta^{2}H$ were collected in 30 mL high density polyethylene (HDPE) bottles and left unrefrigerated (see Gibson et al., 2020). Water samples for analysis of $\delta^{13}C$ in dissolved inorganic carbon (DIC) and dissolved organic carbon (DOC) were field filtered to 0.45um and collected in separate 30 mL HDPE bottles and kept at 4°C and in darkness until they were prepped for analysis.

2.2. Isotopic and geochemical analysis

$\delta^{18}O$ and $\delta^{2}H$ were analyzed at the University of Waterloo during 2002–2008 and thereafter at InnoTech Alberta as described previously (Gibson et al., 2020). Results are provided in "δ" notation in ‰ V-SMOW, where V-SMOW is Vienna Standard Mean Ocean Water. For both labs, analytical uncertainty, estimated as the standard deviation of repeats, has historically been maintained at better than ± 0.2 ‰ for $\delta^{18}O$ and ± 1.0 ‰ for $\delta^{2}H$. $\delta^{13}C$ in DIC and DOC were analyzed on a Delta V Advantage using a GasBench II

peripheral (Assayag et al., 2006). DOC samples were initially acidified and purged with helium to remove any carbonate signature, then an oxidant (sodium persulfate) was added and samples were heated at 80°C for 3 hours, then left to equilibrate overnight before being loaded onto a CTC Analytics autosampler interfaced with the mass spectrometer. For DIC, samples were added to helium-flushed vials which were then acidified for CO_2 equilibration and similarly loaded onto the autosampler for introduction to the mass spectrometer. Results are reported in ‰ V-PDB, where PDB is the PeeDee Belemnite. Analytical uncertainty is estimated at ± 0.3 ‰ for $\delta^{13}C_{DIC}$ and ± 0.4 ‰ for $\delta^{13}C_{DOC}$. Bulk $\delta^{13}C$ in particulate organic matter (POM) was analyzed using a Costech 4010 elemental analyzer connected to a Thermo 253 mass spectrometer via a Conflo IV. Samples were weighed into tin capsules and then dropped into an oxidation reactor packed with chromium oxide and silvered cobaltous/ic oxide (1020°C). Helium carrier gas was then used to entrain the combustion products through a reduction reactor packed with elemental copper (700°C, to scavenge oxygen and reduce NOx products to N_2) before passing through a water trap (magnesium perchlorate), and a column (to separate N_2 from CO_2), and on to the mass spectrometer. Analytical uncertainty for $\delta^{13}C_{POM}$ is estimated at ± 0.2 ‰.

Radon-222 was measured in 37 RAMP lakes in 2010 using a RAD-7 applying a novel canister method (Schmidt et al., 2010). Data were later corrected to ensure comparable readings to the standard 2-L PET pop bottle method (see https://durridge.com/products/big-bottle-system/).

2.3. Geochemical modelling

Saturation indices were determined using the equilibrium/mass-transfer model PHREEQC 3.5.0 (Parkhurst and Appelo, 1999) as presented in Castrillon Munoz et al. (2022). PHREEQC is an equilibrium/mass-transfer model that calculates saturation indices (SI) for discrete mineral phases, thereby predicting whether a mineral is saturated ($SI > 0$) and potentially precipitating or undersaturated and potentially dissolving ($SI<0$). Mann-Kendall was used to predict trends in SI for selected mineral phases as described below.

2.4. Statistical analysis

2.4.1. PCA analysis

Principal component analysis (PCA) is a multivariate statistical technique that transforms and extracts meaningful information from large datasets with many variables. After the data transformation, the first principal component (PC1), a linear combination of the original variables, explains the largest amount of variation in the dataset, and the second principal component (PC2), another linear combination of variables, describes the next largest variation remaining in the dataset, and so on. As the first few principal components (PCs) account for a large part of the variability in the dataset, we can use these PCs to represent the data without losing important information. When presenting PCA results, the projection of individual samples onto the axis defined by a PC is termed the “score”, whereas the coefficient for each variable in the linear combination is called the “loading” of the variable. In this study, we use PCA to transform analytical data to provide enhanced separation for use in visualization of drivers of various variables and to establish likely process linkages. PCA analyses were performed using Sigmaplot versions 14.5 and 15.0.

2.4.2. Mann-Kendall statistics

Mann-Kendall tau and p values, which were applied to assess monotonic trends in climate, water balance and geochemical parameters, were calculated in Microsoft Excel for Microsoft 365® using the MAKESENS freeware template developed by the Finnish Meteorological Institute (Salmi et al., 2002).

2.5. Lake and watershed parameters

Physical characteristics for lakes and their watersheds were based on data summarized in Gibson et al. (2019a). These parameters include: latitude, longitude, elevation, lake area, watershed area, drainage basin area, lake volume, mean and maximum lake depth, drift thickness, and distance to nearest buried channel thalweg. Watershed land cover was delimited by Southern Illinois University (D. Vitt, pers. Comm) using 1:18,0000 black and white air photos following the method of Halsey et al. (2003). While 33 land cover categories were differentiated, including many sub-types of wetlands, our analysis here uses the following major classifications: % bog, % fen, % upland, % open-water and % permafrost. Note that time series information on permafrost extent was unavailable to permit analysis of any trends.

2.6. Climate and water balance analysis

A database compiled by Gibson et al. (2020) summarizes concurrent annual site-specific climate data interpolated for the RAMP lakes during 2002–2017, including Mann-Kendall trend statistics. Climate parameters were adopted from the year-specific 32-km North American Regional Reanalysis (NARR) include 2-m air temperature (T), 2-m humidity (h), and precipitation, evaporation, and evapotranspiration at surface. Estimates of evaporation-flux-weighted air temperature (T_{fw}) and humidity (h_{fw}) are also provided as these were required to run the lake isotope mass balance model (Gibson et al., 2019a) which allowed estimation of residence time (τ) evaporation/inflow (E/I), water yield (WY) and runoff ratio, calculated as WY/P for watershed contributing areas.

2.7. Water yield, runoff and GW/SW

A NARR climatological runoff estimate (RO) from the drainage basin area was approximated from the volumetric flux deficit, P – ET, where P is precipitation and ET is evapotranspiration from the drainage area contributing to the lake, similar to the approach used by Gibson et al. (2022) for open water wetlands. RO was then used as an estimate of surface runoff and WY - RO was used to approximate groundwater contributions to the lakes. These metrics were then combined to estimate the ratio GW/SW for each lake as well as the Mann-Kendall statistics for 2002–2017. Lake-specific data including hydrochemical and isotopic analysis results as well as Mann-Kendall statistics are provided as Supplementary Material.

2.8. Trend visualization graphs

As it is a challenging task to summarize trends and illustrate them systematically for large datasets, we developed a customized graph style for this purpose. Our dataset includes 50 lakes and 25 variables which would require 1250 individual plots to illustrate them directly, not to mention additional plots required to interrogate differences in various sub-groupings, including differentiation by watershed type and by thaw status (or equivalent of 12,500 individual plots). Our solution (see Fig. 3) was to plot water quality variables on the x-axis and the distribution of Mann Kendall tau statistics, *via* box plots, on the y-axis. Mann-Kendall p values for the correlations are provided in the supplementary material. Box plots capture the trend variability (including 5th, 25th, 75th, 95th percentiles) among lakes and median values illustrate normal observations, either positive or negative. Colours are used to differentiate the magnitude of trends in variables (according to median values) for various groups of lakes, for visualization purposes. Trend magnitude is also highlighted using colour-coded box fills (see Fig. 3 legend), using arbitrary limits for illustration. Note that the initial order we show for water quality variables (x-axis) is according to trend strength among variables overall for all lakes, as a group. For comparative purposes, other sub-groupings retain the same order of water quality variables on the x-axis, but are colour-coded by MKtau ranges, so that significantly different trend behaviours of individual variables can be observed by inspection. Complimentary descriptions of the dominant patterns are also described in the accompanying text.

3. Results

3.1. Evidence of geochemical trends

Box plots are provided to illustrate the range and direction of systematic shifts in geochemical variables for the lakes overall, for subregion groups, and for type classes including bog dominated plateau, fen dominated plateau, and fen dominated lowlands (Fig. 3). Bogs and fens are both peatlands, but are generally differentiated by their water sources; fens having sustained groundwater inputs, whereas bogs are often ombrotrophic (precipitation-fed) and permafrost-rich in many areas. Peatland succession studies have described a genetic relationship between these landforms whereby collapse of bogs often leads to fen development (see Vitt et al., 1994; 2000).

Overall, the most pronounced positive MK tau values, indicating positive trends are found for pH, HCO_3^-, and turbidity. Weaker positive trends were found for Chlorophyll, DIC, Ca, Alkalinity, Mg, and K. No change was noted for SBC, Na, Colour, Aluminium, TSS, NO_2NO_3, DOC, and conductivity. Pronounced negative MKtau values, indicating negative trends were found for Cl, SO_4, TKN whereas weaker negative trends were noted for NH_4, TKN, TP, DP, While these patterns emerge on average, it is important observe the wide range in response illustrated by the box plots and outliers.

Note that significance of monotonic trends was determined based on the threshold of $p < 0.05$. For pH, 46 of 50 lakes had increasing trends, 26 of 50 lakes met the significance criteria of $p < 0.05$, 20 lakes were found to have increasing trends but $p > 0.05$. One lake, BM5 was found to have no trend, whereas NE9, NE10, and SM6 were found to have decreasing trends, although none were significant. NE9 and NE10 are also hardwater lakes with pH greater than 8, where calcium carbonate may in fact be precipitating (see Castrillon et al., 2022) For other strongly increasing parameters, HCO_3^- and turbidity, 35 % of trends were significant at $p < 0.05$ level. For weak trending parameters, including DIC, CA, Mg, K, Alk, chlorophyll, 20 % of trends were significant at $p < 0.05$. Trends assessed as stable or unchanged had 14 % significant, whereas significance for weak and strong negative trends was 18 and 17 %, respectively.

Overall, saturation indices (Fig. 4) reveal weak increasing trends in carbonate mineral saturation and decreasing trends in evaporite mineral saturations (anhydrite, gypsum and halite). Increases in carbonate saturation suggest increasing trends in dissolved solid species in solution (HCO_3, DIC, Alkalinity, Mg). Likewise, decreasing trends in evaporite species indicate reduction in levels of Na, Cl, and SO_4. Note that Ca is a common ion for carbonate minerals as well as anhydrite and gypsum which has been shown to cause increased calcite saturation, or in some cases, precipitation of calcite in geologic settings with gypsum (Li et al., 2010). The carbonate patterns appear to be driven by responses in Shield, Birch Mountains and Caribou Mountains, the latter two containing significant permafrost, in contrast to weak trends in West McMurray, NE McMurray, and Stony Mountains. When looking at lakes by subtype, it is clear that similar trends in SI appear to be occurring in both BDP and FDL but we attribute these to separate causes. For BDP, permafrost thaw is dominant and deep groundwater exchange is inherently limited by impermeable Colorado Group shales, whereas FDL has limited residual permafrost but higher potential for deep groundwater exchange. In fact many FDL lakes are hardwater lakes.

We note the regional importance of evaporite minerals (Anhydrite, Halite, Gypsum) due to presence of the Prairie evaporite and the known dissolution mechanism related to glaciogenic recharge and subsequent reflux which continues to drive saline discharge in springs along the Athabasca and Clearwater River valleys (Grasby and Chen, 2005), also noted for some lakes and fens situated along the salt scarp (Cowie et al., 2015). Relaxation of influence from these sources due to increased flushing by permafrost thaw, meteoric

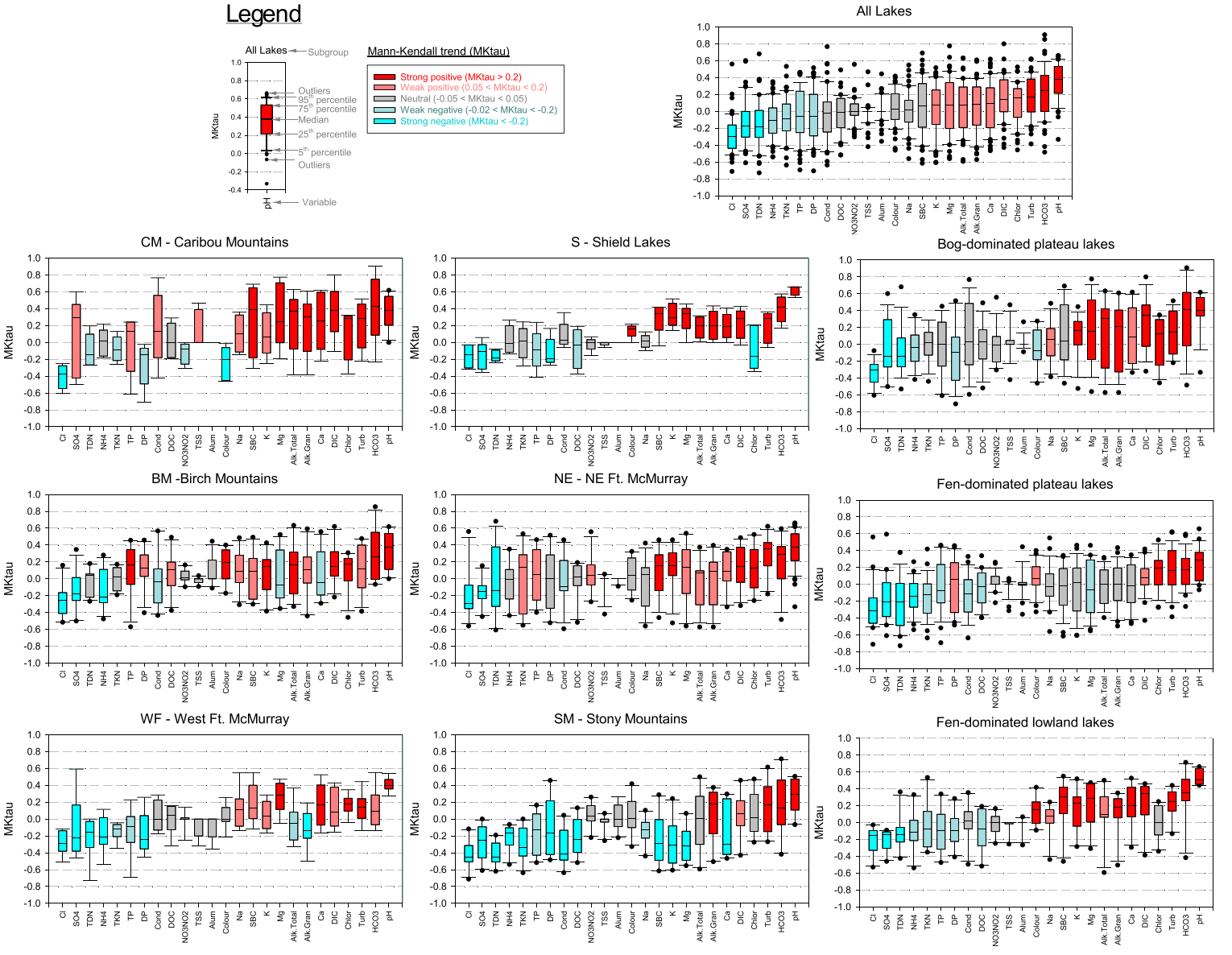

Fig. 3. Geochemical variable trends in RAMP lakes determined from Mann-Kendall analysis for various lake groupings, including: all lakes, lakes by subregion, and lakes by type (bog dominated plateau, fen dominated plateau, fen-dominated lowland). See legend for explanation of box ranges and colours. A detailed description of this graph style as a visualization tool is provided in Section 2.8. See also additional discussion in the text.

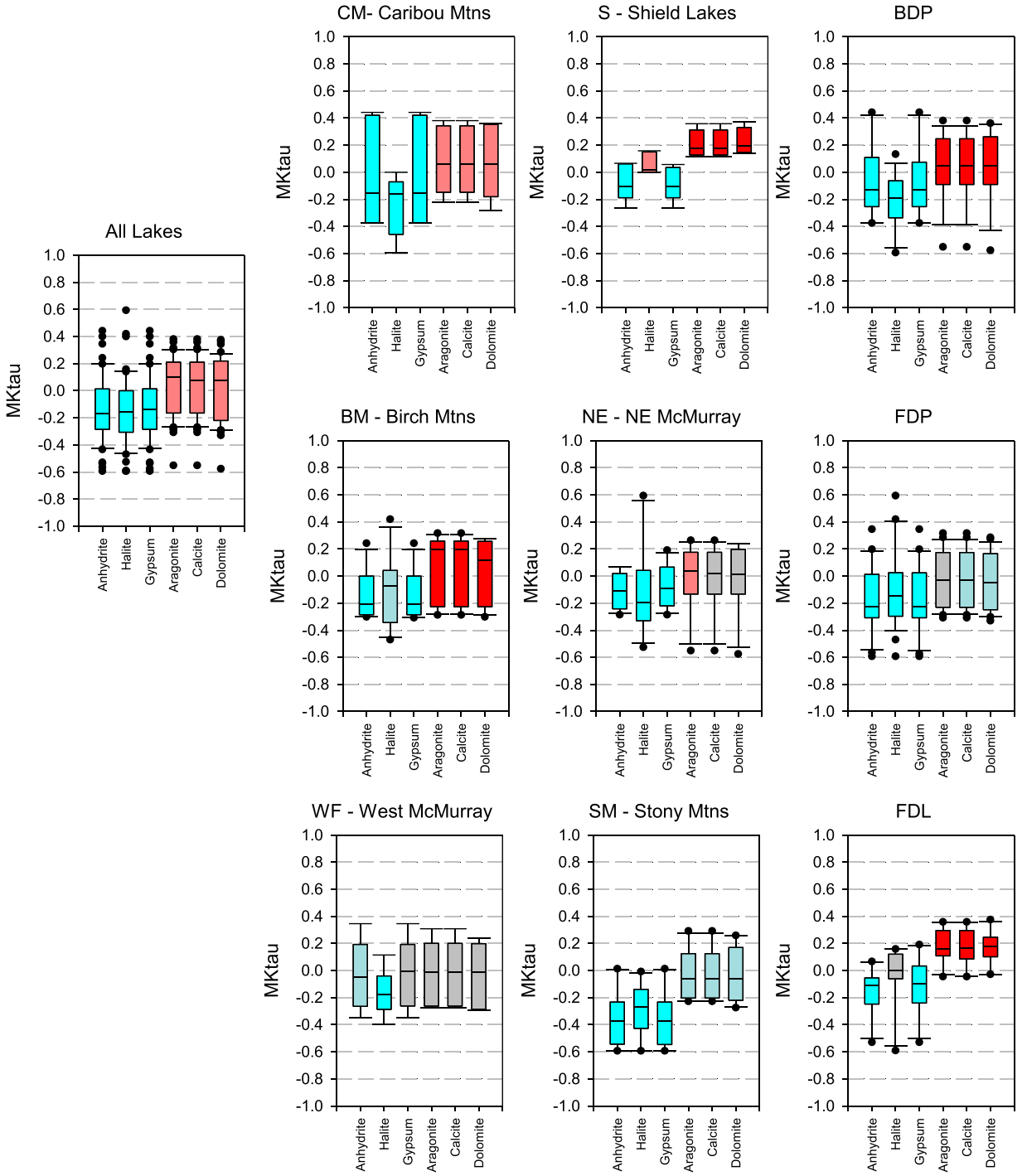

Fig. 4. Mann-Kendall trends in PHREEQC modelled saturation indices for selected mineral phases assuming equilibrium with site-specific RAMP lakewaters. Results are provided by group including: All lakes, lakes by subregion, and lakes by type (bog dominated plateau, fen dominated plateau, fen-dominated lowland). See legend in Fig. 3 for explanation of box ranges and colours. A detailed description of this graph style as a visualization tool is provided in Section 2.8. See also additional discussion in the text. Boxes indicate the median and 25th and 75th percentiles, whiskers indicate the 10th and 90th percentiles. Individual outliers are shown. See text for discussion.

water or fresh groundwater may ultimately explain trends toward declining saturation indices of the evaporite minerals.

Additional modelled parameters including pCO_2, carboxylic acid (A^-), HCO_3, and acid neutralizing capacity (ANC) are also presented (Fig. 5). Overall, decreasing trends are noted for pCO_2 which is observed ubiquitously in all subregions and types. This contrasts

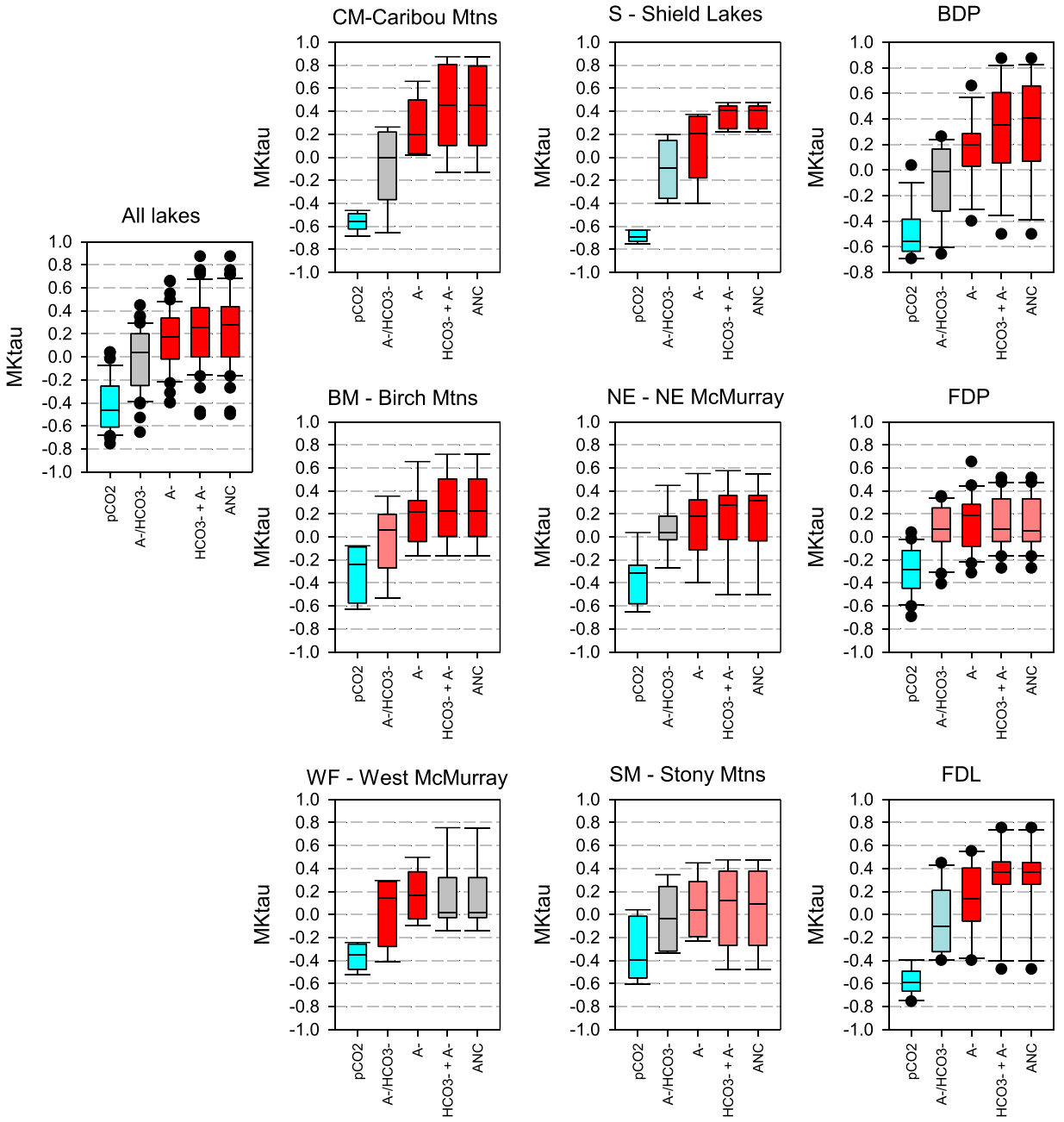

Fig. 5. PHREEQC modelled geochemical indicator trends for RAMP lakes determined from Mann-Kendall analysis. Results are provided by group including: All lakes, lakes by subregion, and lakes by type (bog dominated plateau, fen dominated plateau, fen-dominated lowland). See legend in Fig. 3 for explanation of box ranges and colours. A detailed description of this graph style as a visualization tool is provided in Section 2.8. See also additional discussion in the text. Boxes indicate the median and 25th and 75th percentiles, whiskers indicate the 10th and 90th percentiles. Individual outliers are shown. See text for discussion.

with observations of trends in lakes and streams for other boreal regions, although not in the permafrost-affected zone (Nydahl et al., (2020). While this remains to be confirmed by direct measurements of pCO_2, modelled values suggest widespread supersaturation across the region, with trends toward relaxation to saturation mostly occurring.

Because alkalinity is comprised of both ionized carboxylic acids, (A^-), particularly important in low pH, organic rich lakes, as well as bicarbonate,(HCO3-) we show these parameters as well as A-/HCO3- as an indicator of relative balance of these alkalinity sources. Almost universally, alkalinity is shown to be increasing on average in all settings (with the exception of West McMurray) and the A/HCO3 ratio is found to be mostly stable or weakly trending either positive or negative. Interestingly increases in alkalinity are somewhat weaker for permafrost free subregions (West McMurray and Stony Mountains) as well as largely permafrost free FDP.

3.2. Evidence for trends in climate

For most annual climate variables, positive MKtau values are noted which is broadly consistent with regional warming (Fig. 6). Overall, the strength of the MKtau trends in annual climate variables are, as follows:

E > T > h > P

whereas flux-weighted (evaporation-season) parameters are, as follows:

Tfw > hfw

Among subregions, MKtau trends reveal north-to-south latitudinal shifts, as follows:

Caribou Mtns. > Birch Mtns. = NE McMurray > West McMurray > Stony Mountains

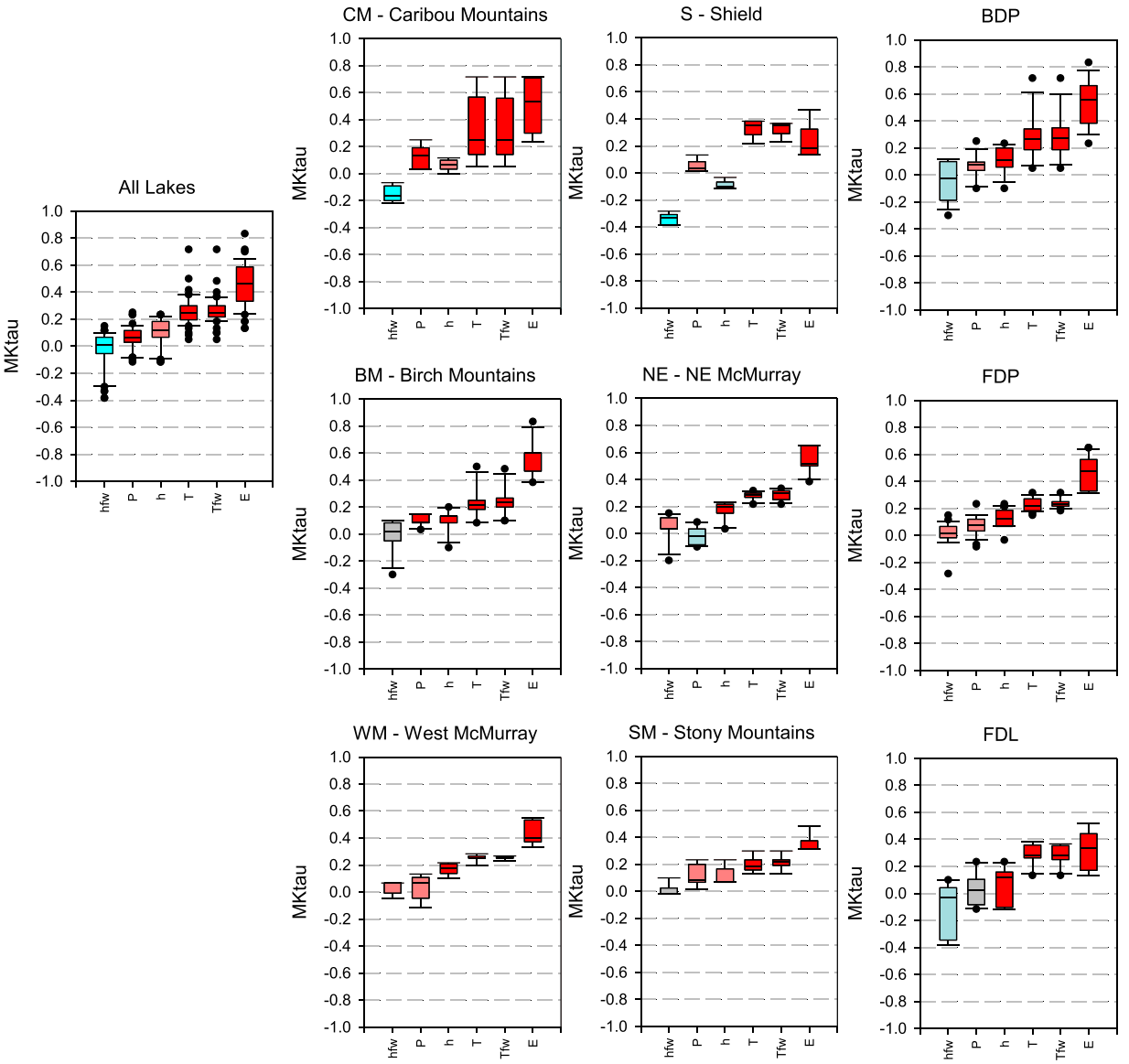

Fig. 6. Trends in interpolated climate parameters for RAMP lakes determined from Mann-Kendall analysis. Results are provided by group including: All lakes, lakes by subregion, and lakes by type (bog dominated plateau, fen dominated plateau, fen-dominated lowland). See legend in Fig. 3 for explanation of box ranges and colours. A detailed description of this graph style as a visualization tool is provided in Section 2.8. See also additional discussion in the text. Boxes indicate the median and 25th and 75th percentiles, whiskers indicate the 10th and 90th percentiles. Individual outliers are shown. See text for discussion.

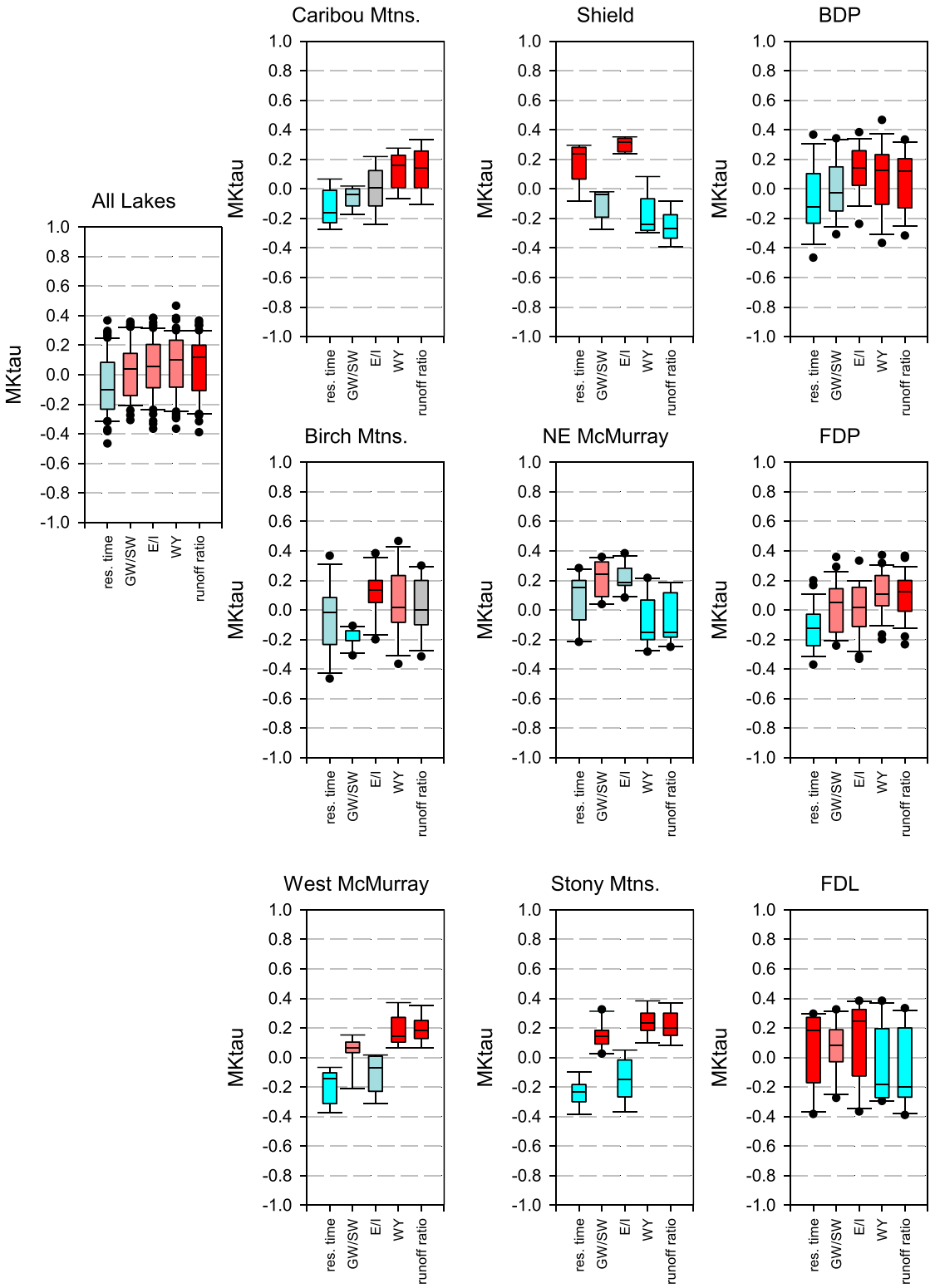

Fig. 7. Trends in isotope-based water balance indicators for RAMP lakes determined from Mann-Kendall analysis. Results are provided by group including: All lakes, lakes by subregion, and lakes by type (bog dominated plateau, fen dominated plateau, fen-dominated lowland). See legend in Fig. 3 for explanation of box ranges and colours. A detailed description of this graph style as a visualization tool is provided in Section 2.8. See also additional discussion in the text. Boxes indicate the median and 25th and 75th percentiles, whiskers indicate the 10th and 90th percentiles. Individual outliers are shown. See text for discussion.

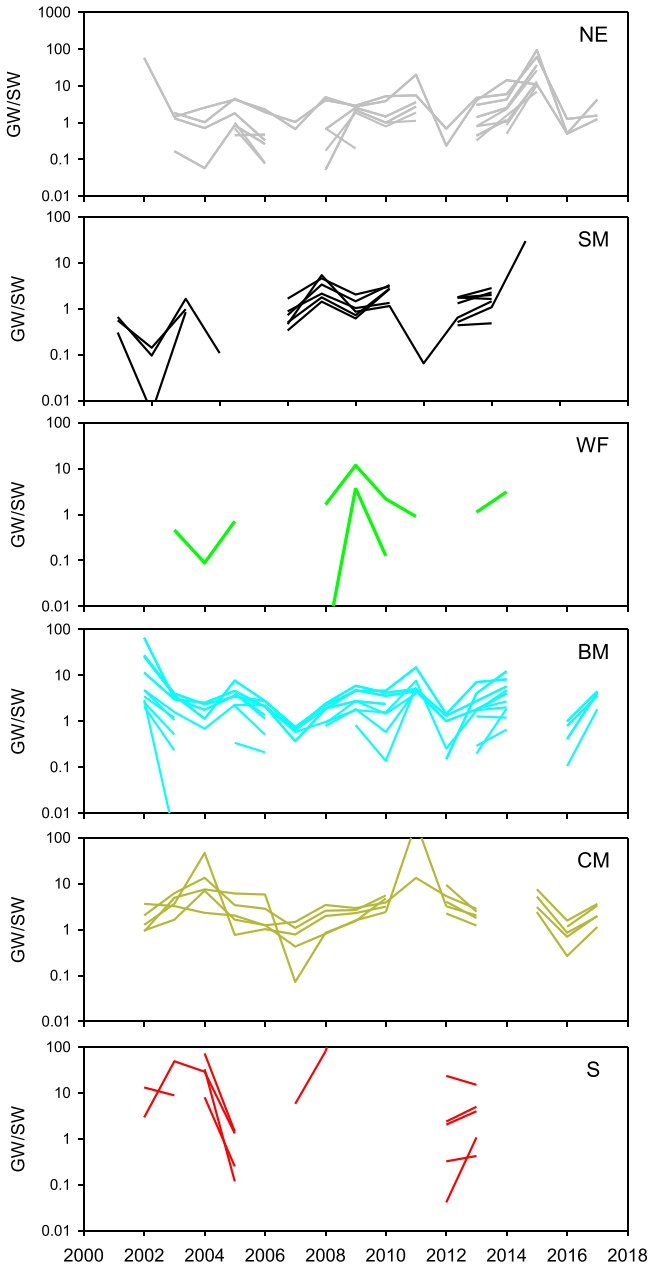

Fig. 8. Calculated annual groundwater/surface water ratios (GW/SW) for individual lakes, grouped by subregion, based on isotope mass balance of lakes applying the partitioning model of Gibson et al. (2022) developed for Alberta open-water wetlands.

Somewhat unique behavior is found for Shield Regions which had positive MKtau for E and T increases but negative MKtau values for humidity, most prominently during the evaporation season. Drier conditions in summer could be result of higher evaporation combined with fundamental differences between boreal plains and boreal shield, the latter characterized by shallow, discontinuous organic soils, and abundance of outcrop, affecting summer aridity.

By type, shield lakes strongly influence patterns in the FDL group which show similar aridity effects, prevalent for humidity during the evaporation season (hfw). Overall, similar trends are noted among all types, although E, T trends are as follows:

$BDP > FDP \approx FDL$

3.3. Evidence for trends in water balance

Water balance is unquestionably driven by climate variables but due to non-monotonic trends in response to permafrost degradation, as reported by Gibson et al. (2019a) for the RAMP lakes, and reported for thermokarst lakes elsewhere (Wan et al., 2019a, 2019b, 2020), the observed trends are apparently more complex for some indicators (Fig. 7).

Overall, positive trends in variables are noted with strength generally varying as follows:

Runoff ratio > WY > E/I > GW/SW

whereas residence time trends are found to be declining for sub-regions or subtypes where thaw sources are on the rise and increasing for post-thaw systems.

The most significant differences are in type categories. Similar responses for BDP and FDP are noted, reflecting higher evaporation losses from lakes but also higher WY and runoff ratios due to permafrost thaw in these plateau areas, and reduced residence times due to related flushing. These influences also appear to dominate in the CaribouMountains and Birch Mountains, which show similar responses. FDL (which have more limited permafrost and therefore more limited permafrost thaw effects) show higher variability, but on average have reduced WY and runoff ratios, and increased residence times. Similar responses for most southerly subregions that are already largely permafrost free, i.e. West McMurray and Stony Mountains. Moderate decreases in residence time and E/I and increases in WY and runoff ratio must be related to increased P and possibly due to enhanced groundwater exchange, evidence of which is described later on.

Different than the northern plateaus, both of the eastern subgroups (NE McMurray and Shield Lakes) are found to have higher E/I and residence times and reduced WY and runoff ratios, which both show similarity to FDL. This appears to reflect that these regions have passed peak WY due to permafrost thaw and are in the recession stages of the thaw cycle.

3.4. Evidence of trends in groundwater exchange

3.4.1. GW/SW ratios

Estimates of GW/SW (Fig. 7) illustrate plausible impact of permafrost thaw on watershed groundwater flowpaths. Lakes are shown on average to be undergoing moderate increases in GW/SW over the course of this study although both positive and negative trends are observed for various lake groups and subtypes. By examining the GW/SW responses among watershed subtypes the influence of permafrost thaw becomes more apparent. On average, BDP watersheds appear to have declining GW/SW which is attributed to reduction in %permafrost up to and perhaps slightly beyond the tipping point of 50 % land-surface cover observed in previous studies (see Gibson et al., 2015; Wan et al., 2019a). On average, slight increases in GW/SW for FDP and FDL reflect additional groundwater interaction with lakes once bogs have extensively collapsed and coalesced to form fens. Subregions CM and BM tend to follow the pattern of BDP whereas NE, WM and SM show similarity to FDP/FDL. A weak but uniform decline in GW/SW is noted for all shield (S) watersheds, similar to BDP.

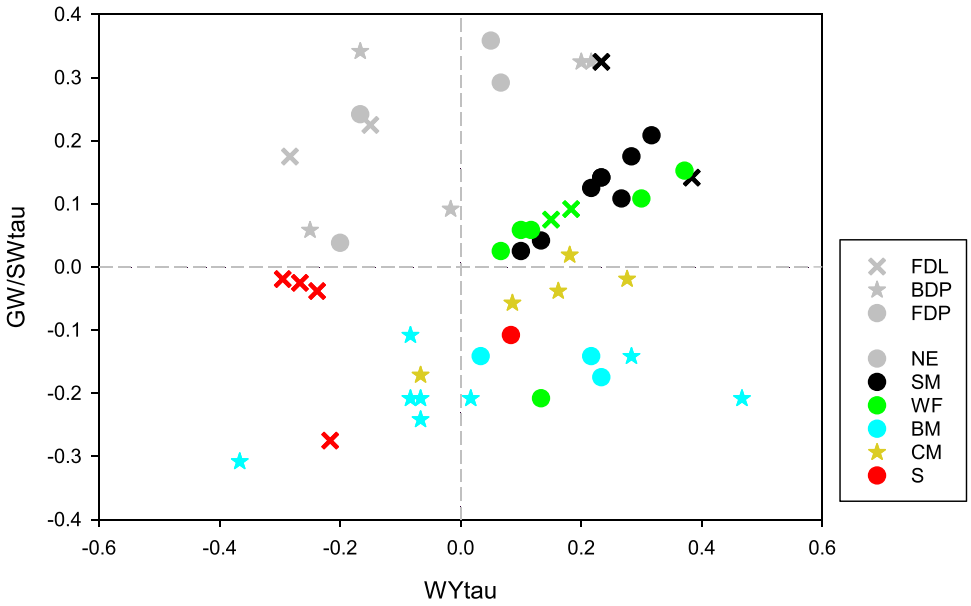

Fig. 9. Crossplot of GW/SWtau and WYtau based on Mann-Kendall statistics for individual lakes, colour-coded by lake subgroup. Note positive correlations for most groups with the exception of Shield lakes (S-red). Positive trends and high correlations are noted for the post-thaw sub-regions (WF-green, SM-black).

To further investigate temporal trends in groundwater exchange, we used Mann-Kendall tau to illustrate annual GW/SW changes by lake/sub-group (Fig. 8) and to explore the potential dependency between GW/SWtau versus WYtau (Fig. 9). While many individual annual values of estimated GW/SW are not shown in Fig. 8 as they were not significant at the $p < 0.05$ level, the interannual trends were found to be systematic and showed clustering by lake subgroup (Fig. 9).

Positive correlations are noted between GW/SWtau and WYtau with the exception of Shield regions. Correlations are strongest for southern subregions with little permafrost, WF, $r^2 = 0.94$; SM, $r^2 = 0.66$ (excluding outliers), and some lakes in NE (r^2=0.37), indicating that unfrozen conditions have likely led to enhanced groundwater exchange with lakes. Despite positive correlations between GW/SWtau and WYtau (CM, r^2=0.78; BM, r^2=0.23), GW/SWtau is predominantly negative for the northern subregions where permafrost is prevalent, consistent with these watersheds being on the rising limb of the thaw trajectory. NE is the only region that has negative WYtau (i.e., falling limb of the thaw trajectory) yet has positive GW/SWtau in areas without permafrost, enhanced there by absence of Colorado shale. Excluding one outlier, Shield watersheds display a high degree of negative correlation (r^2=0.99) between GW/SWtau and WYtau. This indicates reduction in GW/SW ratio with increased WY, likely reflecting activation of surface pathways due to fill-and-spill mechanisms typically governing runoff in shield areas (Spence and Woo, 2003).

3.5. Evidence of carbon sources

Assessment of DIC sources among RAMP lakes was informed by examination of $\delta^{13}C$ in lakewater compared to presumed sources (Fig. 10). While the annual RAMP monitoring program did not routinely involve measurement of $\delta^{13}C$ in lakewater, $\delta^{13}C_{DIC}$ was measured in all RAMP lakes in 2010, 2020 and 2021. $\delta^{13}C_{DOC}$ was measured in all RAMP lakes in 2021 (Open-water DOC). For comparison, we include data from a survey of shallow upland and wetland soil waters reported by Gibson et al. (2021), which included $\delta^{13}C_{DIC}$ (Terrestrial DIC) and $\delta^{13}C_{DOC}$ (Terrestrial DOC) measured at a site within the Stony Mountains subregion. For lakewater, a significant correlation was found between $\delta^{13}C_{DIC}$ values and log DIC (r^2=0.84), which is consistent with DIC being controlled by carbonate dissolution which potentially introduces new DIC into the system from contact with solid phases that may be present (Castrillon-Munoz et al., 2022). Carbonate sources are mainly associated with carbonate rocks in the region, typically ranging between −5 and + 5 ‰ in $\delta^{13}C_{DIC}$ (Saltzman and Thomas, 2012). Higher $\delta^{13}C_{DIC}$ values and higher DIC is found in the hardwater lakes wherein the dominant DIC species are HCO_3^- and CO_3^{2-} as compared to the softwater lakes wherein the dominant DIC species is CO_2. Reference values are shown for atmospheric CO_2 and reference lines are drawn for ^{13}C of individual DIC species at the measured temperature and

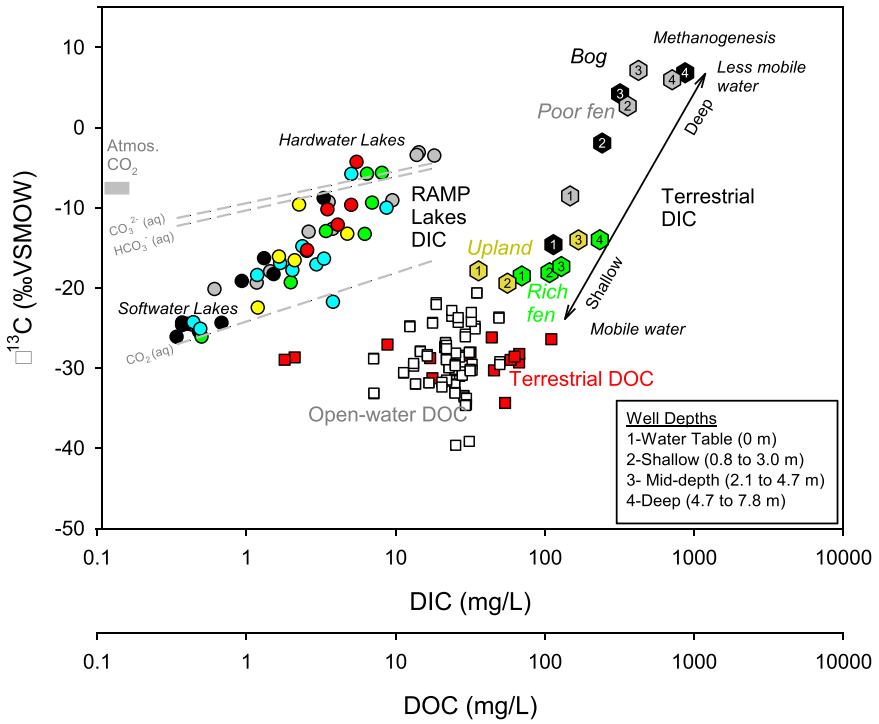

Fig. 10. $\delta^{13}C_{DIC}$ vs. DIC variations in the RAMP Lakes (circles, colour-coded by sub-region), identifying hardwater and softwater endmembers, compared to various potential sources. Numbered hexagons depict $\delta^{13}C_{DIC}$ in DIC of terrestrial soilwaters sampled at a Stony Mountain site Gibson et al. (2021), as colour-coded by terrain type (black – bog, grey – poor fen, green - rich fen, yellow – upland) and numbered according to well-depth range (see legend). For comparison we overlay $\delta^{13}C_{DOC}$ vs. DOC for terrestrial waters (red squares, undifferentiated), and open-water (open circles, undifferentiated). Note that predicted $\delta^{13}C_{DIC}$ solubility curves for carbonate species (CO_2, HCO_3^-, CO_3^{2-}) are approximate, based on measured T, pH, DIC, and $\delta^{13}C_{DIC}$ for all lakes. Hardwater lakes display the highest $\delta^{13}C_{DIC}$ values; softwater lakes display lowest values.

pH of the lakes, based on the Université du Québec à Montréal (UQAM) carbonate speciation calculator (J.F. Helie, pers. Comm.). We note that DIC concentrations were generally several orders of magnitude higher in terrestrial groundwater than in lakewater, with progressive increase observed from rich fens to poor fens to bogs and from surface to depth. Terrestrial DOC from the Gibson et al. (2021) survey was also found to be similar to that of DOC measured in the RAMP lakes. $\delta^{13}C$ above −20 ‰ in RAMP lakes appears consistent with predominance of terrestrial DIC which ranges from −20 ‰ for shallow groundwater from rich fens and uplands to + 10 ‰ for deep groundwater from bogs and poor fens. All but softwater lakes fall within this range (see Castrillon-Munoz et al., 2022). Values of $\delta^{13}C_{DIC}$ for softwater lakes are more consistent with $\delta^{13}C_{DOC}$ in terrestrial sources. $\delta^{13}C_{DIC}$ in hardwater lakes (see Castrillon-Munoz et al., 2022) exceeds values for atmospheric CO_2, and is likely related to presence of carbonate minerals in the lake and/or watershed. Changes observed in $\delta^{13}C_{DIC}$ between 2010 and 2021 are further explored using PCA in the following section. This was not done for $\delta^{13}C_{DOC}$ as this analysis had only been carried out once.

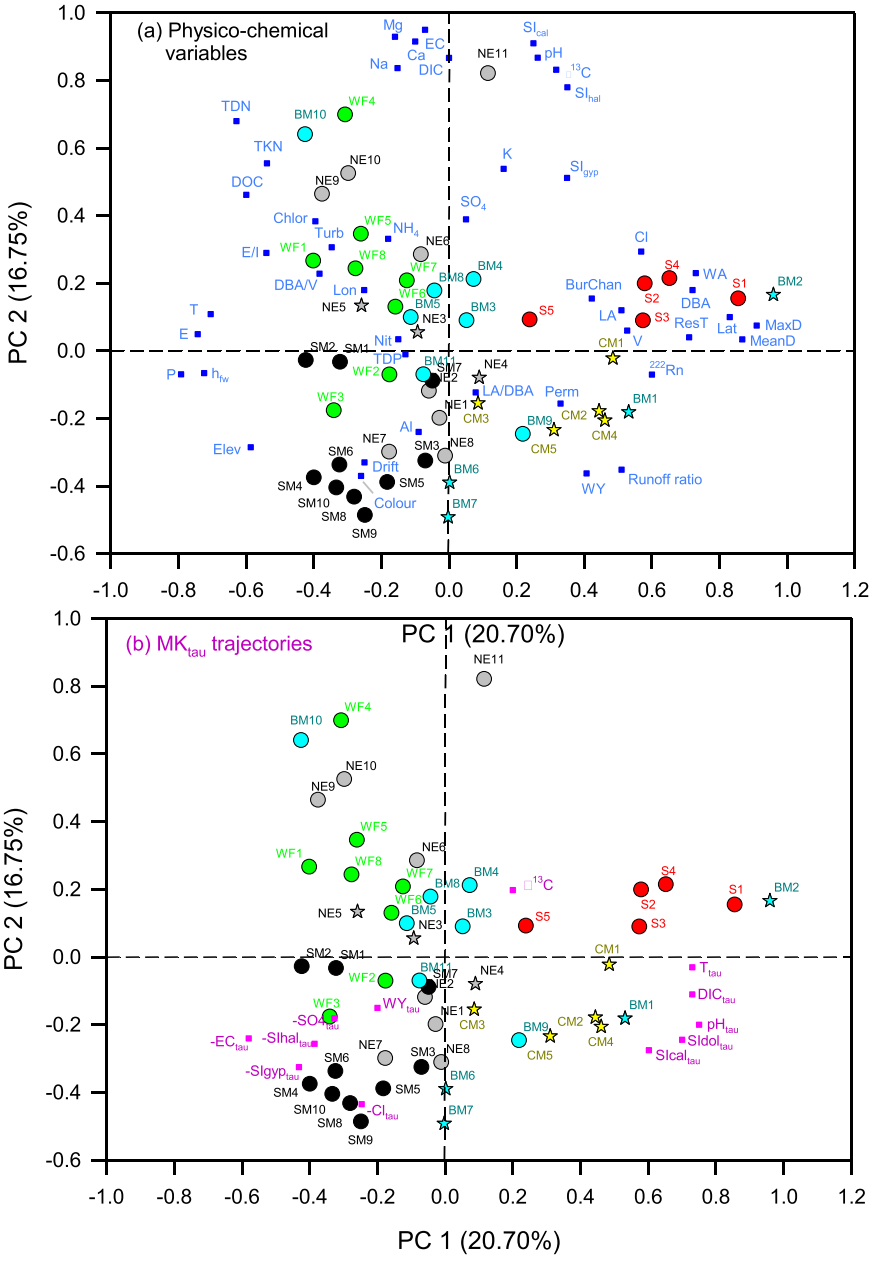

Fig. 11. PCA biplots comparing scores for individual lakes, showing (a) primary loadings variables, and (b) MKtau trajectories of change (+ or -). Note that $\Delta^{13}C$ is calculated as difference between 2013 and 2021 $\delta^{13}C$ values. Star symbols indicate thaw lakes (see Gibson et al. 2019a).

3.6. Relationships between physico-chemical drivers

PCA analysis was used to assess inter-relationships between physico-chemical properties of the RAMP lake network, and to assess various possible mechanisms or drivers controlling the variations among subregional groups and lake subtypes. PCA biplots are shown (Fig. 11) illustrating scores and loadings for the first two principal components (PC1 and PC2), with lakes differentiated by sub-region based on colour (see legend, Fig. 9). Note that similarity between lakes can be judged by their proximity on the plots, which indicate similar scores. Lakes plotting near the origin tend to have near-average geochemical profiles whereas lakes offset significantly from the origin are geochemically distinct. Primary loading variables (Fig. 11a) illustrate the main drivers of variation across the network.

For the RAMP lakes, negative shifts along PC1 are mainly driven by climate variables, including E, T, P, hfw whereas positive shifts appear to be driven predominantly by physical characteristics of the lakes or their watersheds, including LA, WA, DBA, V, MeanD, MaxD, and distance to buried channel (BurChan). ResT, which is strongly dependent on V, and ^{222}Rn, an indicator of groundwater input, also falls along this axis. Positive offset along PC2 appears to be strongly driven by major ions, Ca, Mg, Na, as well as EC and DIC, pH, SI_{cal}, SI_{hal}, and $\delta^{13}C$. Nutrients such as TKN, TDN, DOC, and NH_4, as well as turbidity, E/I and DBA/V, which pull to the upper left hand quadrant, and SO_4, Cl and SI_{gyp}, which pull to the upper right hand quadrant, may also contribute to positive offset along PC2. Negative shifts along PC2 below the origin appear to be the product of properties such as Al, colour, and drift thickness (Drift), which pull to the lower left-hand quadrant, and %permafrost, runoff ratio and WY, which pull to the lower right hand quadrant. Shield lakes are found to cluster along the positive PC1 axis, mainly reflecting their large areas (both lake and watersheds), larger than average depths and volumes, and long residence times. Permafrost thaw lakes, which are largely bog-dominated, including lakes from the Caribou Mountains, Birch Mountains, and NE3, are found to cluster mainly in or near the bottom right quadrant. BM2 (Namur Lake) is a very large lake and appears to respond to some of the same physical drivers which influence. Shield Lakes. Lakes NE3 and NE5, which are also thaw lakes but are nutrient rich, plot in the upper left quadrant but close to the origin. In general, fen-dominated lakes including SM and WF lakes and most NE lakes without significant permafrost in their watersheds generally plot in the upper left quadrant, if nutrient rich or hardwater lakes, and in the lower left quadrants, if lakes are nutrient poor and dilute. Note that NE 11 is Kearl Lake, which was a hardwater lake prior to being developed as an open-pit mine.

3.7. Drivers of pH change

Selected Mann-Kendall tau values (MK_{tau}) were also included in a separate PCA analysis to illustrate and overlay the major tendencies of change, to identify key variables that may be causing the changes, and to explore how such changes may affect some lakes more than others. By inspection, we see that MK_{tau} values for specific physico-chemical variables (Fig. 11b) do not generally align with the variables themselves (Fig. 9a), a finding which is not surprising given that this is similar conceptually to the relationship between velocity and acceleration. This is instructive for how the trends and the trend drivers are interpreted. For example, T is negatively correlated with Lat, as higher temperatures are generally found at lower latitudes, although T_{tau} is positively correlated with latitude, as temperature changes are occurring more rapidly at higher latitudes.

Loading of WY *versus* WY_{tau} drivers is more difficult to interpret however, as we have previously shown that changes in WY are expected initially to increase in watersheds undergoing permafrost thaw but that WY is expected to reduce as permafrost extent is reduced below 50 %, in accordance with the described permafrost thaw cycle (Gibson et al., 2019a). This limits the strength of any monotonic trends in WY and resulting in WY_{tau} being less influential and plotting close to the origin.

For MK_{tau} drivers plotting in the lower left quadrant (Fig. 11b) including -ECtau, -Cl_{tau}, -$SO4_{tau}$, -$SIhal_{tau}$ and -$SIgyp_{tau}$, we attribute largely negative MK_{tau} values with relaxation of glaciogenic influences, owing mainly to permafrost thaw and increased precipitation, although dewatering of drift aquifers and buried channels may also be influential in reducing reflux of saline waters. Lake subgroups that appear to be most affected by such changes, SM, NE, and WF lakes, are characterized by having impermeable shale substrates but situated proximate to buried channels, being fairly dilute, and being further along the permafrost thaw trajectory.

From Fig. 11b, we find that most of the other trend drivers cluster in the lower right quadrant. Drivers in the lower right quadrant, which align with groupings for the thaw lakes, include pH_{tau}, T_{tau}, DIC_{tau}, $SIdol_{tau}$, and $SIcal_{tau}$, As noted, primary variables driving variation in the lower right quadrant include ^{222}Rn, WY, runoff ratio along with a weak influence of LA/DBA. These results are consistent with findings of Gibson et al. (2019a) who showed that lakes receiving significant runoff derived from permafrost thaw also typically had higher isotope-based WY and higher runoff ratios. Alignment of pH_{tau}, DIC_{tau}, $SIcal_{tau}$, $SIdol_{tau}$, with WY, runoff ratio and ^{222}Rn strongly imply that these drivers are causally related.

Based on difference between $\delta^{13}C_{DIC}$ in 2010 and 2021, rather than MK_{tau} derived from a time-series, $\Delta^{13}C$ was found to be positive for 43 of 50 lakes, which might be evidence for geogenic over biogenic sources of DIC as noted by Campeau et al. (2017), but needs to be verified from trend analysis based on longer term monitoring. Dominance of geogenic sources would be consistent with the hypothesis of bog collapse due to permafrost thaw leading to export of carbon from the watershed to the lake. Unlike $\delta^{13}C$, which is a strong differentiator of hardwater *versus* dilute lakes along PC2, $\Delta^{13}C$ is a weak differentiator on the PCA, as revealed by its proximity to the origin, owing to its near-uniform positivity (Fig. 11b). More complicated carbon cycle changes leading to pH increase may be occurring in the lakes although a more exact diagnosis would benefit from a full inventory of $\delta^{13}C$ in various storage reservoirs and fluxes including methane and dissolved CO_2.

3.8. Prediction of pH

Importance of geochemical variables for prediction of pH changes (pH_{tau}) was also assessed from a best subsets linear regression

Table 1
Selected best subsets regression models describing controls on pH change.

	Model	P	r^2	Equation
	1	< 0.001	0.472	$pH_{tau} = 0.504 \cdot HCO3_{tau} + 0.233$
50 lakes	2	< 0.001	0.644	$pH_{tau} = 0.479 \cdot HCO3_{tau} + 0.071\ (+0.022 \cdot \delta^{13}C - 0.037 \cdot DIC)$
	3	< 0.001	0.682	$pH_{tau} = 0.459 \cdot HCO3_{tau} + 0.745\ (+0.026 \cdot \delta^{13}C - 0.385 \cdot DIC - 0.225 \cdot WY_{tau})$
Sub-regions				
NE	4	0.015	0.788	$pH_{tau} = 0.670 \cdot HCO3_{tau} + 0.549\ (+0.015 \cdot \delta^{13}C - 0.015 \cdot DIC)$
SM	5	0.146	0.683	$pH_{tau} = 0.378 \cdot HCO3_{tau} + 0.272\ (+0.164 \cdot DIC - 0.895 \cdot WY_{tau})$
WF	6	0.007	0.899	$pH_{tau} = 0.805 \cdot HCO3_{tau} + 0.563\ (+0.021 \cdot \delta^{13}C - 0.333 \cdot WY_{tau})$
BM	7	0.003	0.647	$pH_{tau} = 0.605 \cdot HCO3_{tau} + 0.174$
CM	8	0.014	0.901	$pH_{tau} = 0.345 \cdot HCO3_{tau} + 0.281$
S	9	0.034	0.821	$pH_{tau} = 0.331 \cdot HCO3_{tau} + 0.498$
Lake type categories				
BDP	10	< 0.001	0.700	$pH_{tau} = 0.509 \cdot HCO3_{tau} + 0.230$
FDP	11	< 0.001	0.442	$pH_{tau} = 0.602 \cdot HCO3_{tau} + 0.164$
FDL	12	0.001	0.926	$pH_{tau} = 0.207 \cdot HCO3_{tau} + 0.748\ (+0.019 \cdot \delta^{13}C - 0.096 \cdot WY_{tau})$

analysis for the various lake subgroups (Table 1). $HCO3_{tau}$ was found to be the strongest predictive variable for all models tested for all groups, accounting for between 42 % and 93 % of variability in pH_{tau}. In addition, $\delta^{13}C_{DIC}$, DIC, and WY_{tau} were found to moderately improve correlations overall for the 50 lakes, but did not significantly improve the predictive power for plateau lakes including the Birch Mountains (BM) and Caribou Mountains (CM), as well as the Shield (S) lakes.

This analysis further establishes the coupling of changes in pH and HCO_3^-, and as discussed below, explores plausible explanation for the observed trends including the importance of $\delta^{13}C_{DIC}$, DIC, and WY_{tau} in some regional lake settings.

4. Discussion

4.1. Geological controls

Shale dominated or crystalline sub-crop areas with no carbonate, or limited carbonate tend to be well-described by the $HCO3_{tau}$ variable only (e.g., BM, CM, S, BDP, FDP) and correlations tend to improve very little if other variables are considered, whereas for areas with ancient sources of carbon, correlations tend to improve and are responsive to addition of variables that capture these additions including $\delta^{13}C_{DIC}$ and DIC (e.g, NE, SM, WF, FDL). Regression models for sites without permafrost, that are inferred to be largely post thaw (e.g., SM, WF, FDL) also showed improvement if WY_{tau} is considered. This is consistent with water yield responses being dependent on permafrost thaw status, generally increasing until permafrost is 50 % thawed and then decreasing thereafter, as noted by Gibson et al. (2019a). It is important to distinguish the hydrogeological setting of SM lakes as being located entirely within Colorado shale-dominated subcrop areas west of the bitumen edge, areas known from analysis of ^{34}S and ^{18}O in SO_4 to be dominated by pyrite weathering (Birks et al., 2019), whereas areas to the east of the bitumen edge where Colorado shale and bitumen are absent are dominated by SO_4 with evaporitic signatures, and have been attributed to glaciogenic sources upwelling from the Devonian formations (Birks et al., 2019). The geological setting of hardwater lakes (NE9,NE10, NE11) suggests that they are less sensitive to change as they are likely in communication with glaciogenic groundwaters found throughout the McMurray, Clearwater and Grand Rapids formations by (Birks et al., 2019; see their Fig. 5), and are evident as sources for some SAOS lakes.

4.2. Acidifying emissions

The Mann-Kendall analysis showed that 46 of 50 RAMP lakes had monotonically increasing pH, 26 significant at the $p < 0.05$ level. One lake, BM5, a fen-dominated plateau lake, showed no monotonic trend. Among lakes that showed weak decreasing trends in pH, NE9 and NE10 are hardwater lakes, and as such are well-buffered and unlikely to be in jeopardy of acidification. Lake SM6, a fen dominated plateau lake with a pH of 5.42 and a $\delta^{13}C_{DIC}$ of −24.66 ‰, which is dilute and predominantly buffered by carboxylic acids (Castrillon-Munoz et al., 2022), is the only lake which appears to be actively acidifying. This lake has a very low WY (77 mm/yr) compared to an average of 215 mm/year for SM lakes, it has a low runoff ratio (0.13) compared to an average of 0.38 for SM lakes in general. According to the steady state water chemistry model of Henriksen et al. (2002), low water yield and soluble base cations are the principal determinants of critical loads of acidity. From a prior critical loads assessment (Gibson et al., 2010a), SM6 was found to have the lowest critical load among the Stony Mountains Lakes (63 $eq \cdot ha^{-1} \cdot yr^{-1}$) and was sixth most acid sensitive lake among the 50 RAMP lakes. Others that were predicted to be very sensitive had lower critical loads (e.g., S2, S4, BM10, WF3, WF4, WF5, WF8) and all had limited permafrost, although they were not found in our assessment to be actively acidifying, but basifying. The inability of the critical loads model to predict basification, which was only revealed following 2 decades of geochemical monitoring, is a clear shortcoming of the model related to reliance on soluble base cation concentrations to predict pH buffering in the lake, rather than a more comprehensive representation of carbonate equilibria as provided by the PHREEQC model used here and previously by Castrillon-Munoz et al. (2022). However, the critical loads model does appear to capture the potential influence of variations in water yield over the course of the typical permafrost thaw cycle. This thaw cycle is expected to increase water yield early in the thaw process

and then a gradual reduction in water yield as thaw progresses. We can postulate that thawing may buffer acidification early on but reduction in runoff over the long term is expected to enhance acidification potential. Overall, this may imply that the current situation of pH increase will ultimately be weakened or reversed once thawing is complete. Analogues for this situation can be seen in the southern subgroups (SM, WF) which, along with shield lakes (S) appear to be among the most acid sensitive lakes in the region (Gibson et al., 2010a).

4.3. Permafrost thaw, temperature and enhanced carbon input

No time-series information is currently available for the RAMP watersheds that quantifies permafrost extent to establish permafrost degradation, although indirect evidence of ongoing landscape changes can be seen in many cases from satellite and air photo interpretation. Bog collapse and fen collapse due to permafrost thaw (Fig. 1) and permafrost terrain distribution itself were shown to be prominent drivers of regional hydrology in the RAMP region (Gibson et al., 2015) and similar features have been widely observed across the circumboreal and circumpolar regions, as we noted previously. Water cycle changes associated with permafrost thaw were revealed from watersheds inferred to be at different stages along a thaw trajectory (Gibson et al., 2019a). Based on widely reported changes in carbon cycling in watersheds with thawing permafrost (e.g., Kuhn et al., 2021), we also anticipate changes in allochthonous DOC, DIC and POM transport to lakes. We postulate that POC or DOC are not the dominant mechanisms of mineralization as they would expectedly lead to reduction in $\delta^{13}C_{DIC}$ which is not widely found. Furthermore, predicted $\delta^{13}C_{DIC}$ in the lakes is in close agreement to predictions based on carbonate geochemical equilibria (see Fig. 10). One process that is known to enrich $\delta^{13}C_{DIC}$ values is methanogenesis which has not yet been sampled or isotopically characterized in the RAMP lakes.

Temperature of the RAMP lakes was found to be increasing in 40 of 50 lakes, 11 of these at the $p < 0.05$ significance level. Previous workers have noted increasing temperatures both at surface and from less frequent monitoring of near-bottom conditions (Yi, pers. Comm.). Carbonate solubility and related isotopic fractionations are known to be reduced at higher temperatures but would presumably have less effect on hardwater lakes with carbonate present than softwater lakes where $\delta^{13}C_{DIC}$ is anchored mainly by pCO_2. We note that almost all lakes apart from the Shield Lakes are situated on sedimentary platform containing abundant carbonate rocks. Surficial till (a.k.a. glacial drift) containing carbonates is present in almost all of the lakes or watersheds. The fact that $\delta^{13}C_{DIC}$ is apparently increasing in 43/50 lakes suggests dissolution of additional carbonate may be occurring.

4.4. Productivity

Poor correlation between pH, pH_{tau}, DIC, DIC_{tau} or $\delta^{13}C_{DIC}$, or $\Delta^{13}C$ and any of the common productivity indicators such as Chl-a, Nitrate, TDP, TKN, or TDN, suggest that productivity is not a major control on pH trends in the lakes.

4.5. Lake ice changes

Lakes across Boreal Canada have undergone considerable changes in ice-on and ice-off dates as measured over the past few decades. According to Gratton and Bélanger (2018), ice duration for lakes in northern Alberta is expected to decrease on average by 2.75 days/decade, with earlier thawing of ice cover by 2.4 days/decade and delayed freeze-up by 1.85 days/decade. It is predicted that ice thickness will decrease by 2 cm/decade which will be accompanied by reduction in maximum ice thickness by 3.1 cm/decade. The result of reduced duration of ice cover likely has been and will continue to be enhanced CO_2 exchange from lakes,and depending on the status of the carbon cycle and hardness of water, may lead to CO_2 uptake from the atmosphere or enhanced CO_2 efflux (Finlay et al., 2015). Based on PHREEQC modelling in our study, it appears that pCO_2 for the majority of RAMP lakes is decreasing with time, which occurs in lockstep with measured pH increases. While this is a plausible mechanism for pH increase, it is based on modelled rather than field-based measurements, and so remains to be verified as a causal factor in pH changes. Furthermore, the relative importance of atmospheric CO_2 exchange versus terrestrial carbon inputs requires additional field data to evaluate.

4.6. Plausible attribution to climate changes and permafrost thaw

Evidence of hydrogeochemical trends in typical lakes in northeastern Alberta have been substantively linked to concurrent processes including climate change, water balance trends, alteration of groundwater exchange, ice cover duration, and shifts in carbon sources, which have driven physico-chemical and pH changes in the lakes over two decades of observation. Predictive pH models have also been proposed based on this analysis that serve to differentiate the observed response of lakes in different subregions with differing geological controls. We have provided context for understanding the role of acidifying emissions on the lakes, for appreciating limited impacts due to productivity changes, and we document evidence of trends in permafrost thaw and reduced ice-cover duration and the likely role of these processes in regional carbon cycle modification and pH regulation. Overall, we consider the weight of evidence presented here to constitute plausible attribution of hydrogeochemical changes and near-universal pH increases to recent climate change and to permafrost thaw associated with recent climate change. While impacts related to carbon input to lakes *versus* enhanced CO_2 evasion have yet to be quantitatively partitioned, we conclude that these are the most important controls requiring follow up in future investigations.

Attribution of pH increase to climate changes, including permafrost-thaw-related carbon loading, is consistent with previous lake assessments by Summers al. (2016) who concluded that climate changes were apparently more influential than oil sands deposition on local lakes. It is important to acknowledge other investigations carried out on hardwater lakes, specifically lakes in Saskatchewan

located between 50 and 51°N which revealed that lakes have undergone reduction in pCO_2, while total organic carbon budgets, hydrological budgets and lake productivity have been steady (Finlay et al., 2015). As a result, hardwater lakes have transitioned from being carbon sources during the 1990s to carbon sinks today, with similar increases observed in summer pH related to warmer conditions and reduced ice cover. While we might expect similar controls to prevail for the RAMP lakes, this must only be part of the story given known increases in runoff inputs and related carbon loading due to permafrost thaw. An important distinction is that the RAMP network also includes softwater lakes characterized by organic acid buffering which might be expected to demonstrate greater pH sensitivity due to reduced carbonate buffering. However, differential sensitivity of hardwater and softwater lakes within RAMP is not convincingly supported by $\delta^{13}C_{DIC}$ patterns or by other indicators. For RAMP lakes, we emphasize that strong evidence of changes in inflow and increased groundwater interaction has been found, which may also carry additional carbonate to the lakes. As shown by Kuhn et al. (2021) for a north-south transect of lakes spanning from permafrost to permafrost-free sites, we might also expect lake methane emissions to increase while carbon dioxide exchange decreases moving south, although this has yet to be confirmed for the RAMP lakes.

5. Conclusions

Systematic hydrogeochemical trends over two decades in a network of 50 boreal lakes monitored in northeastern Alberta, Canada are confirmed by Mann-Kendall statistical tests, and underlying causes are investigated and inferred based on a comprehensive array of climate, land cover, and hydrologic indicators, as well as geochemical modelling and isotopic diagnostics. Widespread trends, both statistically significant and non-significant, including increase in pH in 46 of 50 lakes, are substantially attributed to permafrost thaw progression occurring in wetland-dominated contributing areas. WY and WY trends were found to be essential for establishing the thaw status of individual lakes. With the exception of shield lakes, groundwater contributions are generally found to be increasing with water yield and carbon inputs as sites advance across the thaw trajectory. pH control was found to be straightforwardly described by variations in HCO_3^- in shale-dominated bedrock areas, inferred to be the result of allochthonous carbon input and regulation, whereas pH was also influenced by presence of carbonate minerals in some lakes, as revealed by improved prediction of pH when DIC and $\delta^{13}C_{DIC}$ were considered. We postulate that recent pH trends across the region may only be temporary and that lake acidification may yet occur once permafrost thaw and related carbon imports diminish.

Due to reliance on one-time in-lake sampling in late summer/fall, our description of the hydrogeochemistry has essentially focused on systematic responses at the regional scale, which limits its value for assessing processes associated with thawing and carbon release which originate within the watersheds. Detailed process studies at selected sites along the thaw trajectory would be advantageous to improve description and understanding of water and carbon release mechanisms. Within the constraints of the program, our efforts in 2022 allowed for collection of additional water samples for $\delta^{13}C$ in particulates (POM), dissolved solids (DIC, DOC) and dissolved gases (CH_4, CO_2) to improve understanding of the carbon release processes and regulation of pH, as much as practical, based on in-lake measurements. Samples were also collected for future analysis of environmental DNA (eDNA) with a view to documenting potential changes in ecosystem diversity and function accompanying pH and hydrogeochemical changes across the regional thaw trajectory.

Our research potentially offers broader insight into the periodic nature of permafrost thaw and its anticipated impacts that need to be considered for resource impact assessments in cold regions due to widespread degradation of permafrost under current climate conditions.

Declaration of Competing Interest

The authors declare that they have no known competing financial interests or personal relationships that could have appeared to influence the work reported in this paper.

Acknowledgements

Alberta Environment and Parks provided access to monitoring data and in-kind support for logistics and sample analysis. Non-routine analyses including isotopic tracers was funded via grants to JJG from InnoTech Alberta and its predecessors, the Cumulative Environmental Management Association, and the Natural Sciences and Engineering Research Council of Canada. Coordination and logistical support was provided by Preston McEachern, Rod Hazewinkel, Colin Cooke, Jean Birks, Yi Yi, and numerous other field staff of AEPA. We thank Paul Eby and staff of University of Waterloo Environmental Isotope Lab for skillful analytical support on isotopes. Mike Moncur assisted with correcting the Radon-222 values for consistency with the widely used Durridge 2-L pop bottle method.

Appendix A. Supporting information

Supplementary data associated with this article can be found in the online version at doi:10.1016/j.ejrh.2025.102253.

Data availability

included as supplementary material

References

Alberta Environment, 2002. Water Quality Sampling Methods. Water Monitoring Group, Compliance Branch, Regional Services, Alberta Environment.

Alberta Environment, 2006. Aquatic Ecosystems Field Sampling Protocols. ⟨https://open.alberta.ca/publications/077855080x⟩.

Alexander, A.C., Chambers, P.A., 2016. Assessment of seven Canadian rivers in relation to stages in oil sands industrial development, 1972–2010. Environ. Rev. 24, 484–494. https://doi.org/10.1139/er-2016-0033.

Assayag, N., Rive, K., Adler, M., Jezequel, D., Agrinier, 2006. Improved method for isotopic quantitative analysis of dissolved inorganic carbon in natural water samples. Rapid Commun. Mass Spectrom. 20, 2243–2251.

Beilman, D.W., Vitt, D.H., Halsey, L.A., 2000. Localized permafrost peatlands in western Canada: definition, distributions, and degradation. Arct., Antarct., Alp. Res. 33, 70–77.

Bennett, K.E., Gibson, J.J., McEachern, P., 2008. Water yield estimates for critical loadings assessment: comparisons of gauging methods vs. an isotopic approach. Can. J. Fish. Aquat. Sci. 65, 83–99. https://doi.org/10.1139/7-155.

Berryman, S., Birks, S.J., Gibson, J.J., Straker, J., Vile, M., Vitt, D., Watmough, S., Wieder, K., 2016. Nitrogen critical loads five-year final report: bog, poor fen, and jack-pine ecosystems, May 2016. Technical Report Prepared for Cumulative Environmental Management Association. Wood Buffalo Region, Alberta, p. 201.

Birks, S.J., Moncur, M.C., Gibson, J.J., Yi, Y., Fennell, W.J., Taylor, E.B., 2018. Origin and hydrogeological setting of saline groundwater discharges to the Athabasca River: Geochemical and isotopic characterization of the hyporheic zone. Appl. Geochem. https://doi.org/10.1016/j.apgeochem.2018.09.005.

Birks, S.J., Fennell, J.W., Gibson, J.J., Yi, Y., Moncur, M.C., Brewster, M., 2019. Using regional datasets of groundwater isotope geochemistry to evaluate conceptual models of groundwater flow in the Athabasca Region. Appl. Geochem. 101, 140–159. https://doi.org/10.1016/j.apgeochem.2018.12.013.

Bonsal, B.R., Peters, D.L., Seglenieks, F., Rivera, A., Berg, A., 2019. Changes in freshwater availability across Canada. Can. 'S. Chang. Clim. Rep. 261–342.

Campeau, A., Wallin, M.B., Giesler, R., Lofgren, S., Morth, C.M., Schiff, S., Bishop, K., 2017. Multiple sources and sinks of dissolved inorganic carbon across Swedish streams, refocusing the lens of stable C isotopes. Sci. Rep. 7, 9158. https://doi.org/10.1038/s41598-017-09049-9.

Castrillon-Munoz, F.J., Gibson, J.J., Birks, S.J., 2022. Carbon dissolution effects on pH changes of RAMP lakes in northeastern Alberta, Canada. J. Hydrol.: Reg. Stud. 40, 101045. https://doi.org/10.1016/j.ejrh.2022.101045.

Cooke, C.A., Kirk, J.L., Muir, D.C., Wiklund, J.A., Wang, X., Gleason, A., Evans, M., 2017. 2017. Spatial and temporal patterns in trace element deposition to lakes in the Athabasca oil sands region (Alberta, Canada). Environ. Res. Lett. 12, 1240001. https://doi.org/10.1088/1748-9326/aa9505.

Cowie, B., James, B., Mayer, B., 2015. Distribution of total dissolved solids in McMurray Formation water in the Athabasca Oil Sands region, Alberta, Canada: implications for regional hydrogeology and resource development. Am. Assoc. Pet. Geol. Bull. 99, 77–90. https://doi.org/10.1306/07081413202.

Culp, J., Droppo, I.G., di Cenzo, P.D., Aleander, A.C., Baird, D.J., Beltaos, S., Bickerton, G., Bonsal, B., 2021. Ecological effects and causal synthesis of oil sands activity impacts on river ecosystems: water synthesis review. Environ. Rev. 29, 315–327. https://doi.org/10.1139/er-2020-0082.

Curtis, C.J., Flower, R., Rose, N., Shilland, J., Simpson, G.L., Turner, S., Yang, H., Pla, S., 2010. Palaeolimnological assessment of lake acidification and environmental change in the Athabasca Oil Sands Region, Alberta. s1 (Aug. 2010). J. Limnol. 69, 92–104. https://doi.org/10.4081/jlimnol.2010.s1.92.

Devito, K., Creed, I., Gan, T., Mendoza, C., Petrone, R., Silins, U., Smerdon, B., 2005. A framework for broad-scale classification of hydrologic response units on the Boreal Plain: is topography the last thing to consider? -Invited Review. Hydrol. Process. 19, 1705–1714.

Devito, K.J., Hokanson, K.J., Moore, P.A., Kettridge, N., Anderson, A.E., Chasmer, L., et al., 2017. Landscape controls on long-term runoff in subhumid heterogeneous Boreal Plains catchments. Hydrol. Process. 31, 2737–2751 https://dx.doi/10.1002/hyp.11213.

Eum, H.-I., Dibike, Y., Prowse, T., 2017. Climate-induced alteration of hydrologic indicators in the Athabasca River Basin, Alberta, Canada. J. Hydrol. 544, 327–342. https://doi.org/10.1016/j.jhydrol.2016.11.034.

Finlay, K., Vogt, R., Bogard, M., Wissel, B., Tutolo, B., Simpson, G., Leavitt, P., 2015. Decrease in CO_2 efflux from northern hardwater lakes with increasing atmospheric warming. Nature 519, 215–228.

Gibson, J.J., Peters, D.L., 2022. Water and environmental management in oil sands regions. J. Hydrol.: Reg. Stud. 44, 101274. https://doi.org/10.1016/j.ejrh.2022.101274.

Gibson, J.J., Prepas, E.E., McEachern, P., 2002. Quantitative comparison of lake throughflow, residency, and catchment runoff using stable isotopes: modelling and results from a survey of boreal lakes. J. Hydrol. 262, 128–144. https://doi.org/10.1016/S0022-1694(02)00022-7.

Gibson, J.J., Birks, S.J., McEachern, P., Hazewinkel, R., Kumar, S., 2010a. Interannual variations in water yield to lakes in northeastern Alberta: Implications for estimating critical loads of acidity. J. Limnol. 69 (. 1), 126–134. https://doi.org/10.4081/jlimnol.2010.s1.126.

Gibson, J.J., Birks, S.J., Jeffries, D.S., Kumar, S., Scott, K.A., Aherne, J., Shaw, P., 2010b. Site-specific estimates of water yield applied in regional acid sensitivity surveys in western Canada. J. Limnol. 69 (. 1), 67–76. https://doi.org/10.4081/jlimnol.2010.s1.67.

Gibson, J.J., Fennell, J., Birks, S.J., Yi, Y., Moncur, M., Hansen, B., Jasechko, S., 2013. 2013. Evidence of discharging saline formation water to the Athabasca River in the northern Athabasca oil sands region. Can. J. Earth Sci. 50, 1244–1257. https://doi.org/10.1139/cjes-2013-0027.

Gibson, J.J., Birks, S.J., Yi, Y., Vitt, D., 2015. Runoff to boreal lakes linked to land cover, watershed morphology and permafrost melt: a 9-year isotope mass balance assessment. Hydrol. Process. 29, 3848–3861. https://doi.org/10.1002/hyp.10502.

Gibson, J.J., Birks, S.J., Yi, Y., 2016. Higher tritium concentrations measured in permafrost thaw lakes, northern Alberta. Hydrol. Process. 30, 245–249. https://doi.org/10.1002/hyp.10599.

Gibson, J.J., Yi, Y., Birks, S.J., 2019a. Isotopic tracing of hydrologic drivers including permafrost thaw status for lakes across northeastern Alberta, Canada: a 16-year, 50-lake perspective. J. Hydrol. Reg. Stud. 26, 100643. https://doi.org/10.1016/j.ejrh.2019.100643.

Gibson, J.J., Birks, S.J., Moncur, M.C., 2019b. Mapping water yield distribution across the southern Athabasca Oil Sands area: baseline surveys applying isotope mass balance of lakes. J. Hydrol. Reg. Stud. 21, 1–13. https://doi.org/10.1016/j.ejrh.2018.11.001.

Gibson, J.J., Yi, Y., Birks, S.J., 2020. Watershed, climate, and stable isotope data (oxygen-18 and deuterium) for 50 boreal lakes in the oil sands region, northeastern Alberta, Canada, 2002-2017. Data Brief. 29, 105308. https://doi.org/10.1016/j.dib.2020.105308.

Gibson, J.J., Birks, S.J., Yi, Y., Moncur, M.C., Vallarino, A., Kusel, C., Cherry, M., 2021. Hydrology and geochemistry studies in the oil sands region to investigate the role of terrain conductivity in nitrogen critical loads. Water 13, 2204. https://doi.org/10.3390/w13162204.

Gibson, J.J., Eby, P., Birks, S.J., Twitchell, C., Gray, C., Kariyeva, J., 2022. Isotope-based water balance assessment for open water wetlands across Alberta: Regional trends with emphasis on oil sands region. S. J. Hydrol. Reg. Stud. 40, 101036. https://doi.org/10.1016/j.ejrh.2022.101036.

Gosselin, P., Hrudey, S.E., Naeth, M.A., Plourde, A., Therrien, R., Van Der Kraak, G., Xu, Z., 2010. Environmental and Health Impacts of Canada's Oil Sands Industry. Royal Society of Canada, Ottawa, ON, Canada.

Grasby, S.E., Chen, Z., 2005. Subglacial recharge into the Western Canada sedimentary basin – impact of pleistocene glaciation on basin hydrodynamics. Geol. Soc. Am. Bull. 117, 500–514.

Hatfield Consultants Ltd. et al., 2016. Regional Aquatics Monitoring Program in support of the Joint Oil Sands Monitoring Plan, 2015 Final Program Report prepared for Alberta Environmental Monitoring, Evaluation and Reporting Agency, April 2016, 1272p.

Gratton, Y., Bélanger, C., 2018. Alberta Lakes Thermodynamic Modelling. Report No. R1785, INRS-ETE, Québec (QC): 92 p.

Halsey, L.A., Vitt, D.H., Beilman, D., Crow, S., Mehelcic, S., Wells, R., 2003. Alberta Wetlands Inventory Standards Version 2.0. Alberta Sustainable Development, Resource Data Branch, Strategic Corporate Services Division, Alberta Sustainable Resource Development: Edmonton; 1–54.

Henriksen, A., Dillon, P.J., Aherne, J., 2002. Critical loads of acidity for surface waters in south-central Ontario, Canada: regional application of the Steady-State Water Chemistry (SSWC) model. Can. J. Fish. Aquat. Sci. 59, 1287–1295. https://doi.org/10.1139/f02-092.

Holmes, R.M., McClelland, J.W., Raymond, P.A., Frazer, B.B., Peterson, B.J., Stieglitz, M., 2008. Lability of DOC transported by Alaskan rivers to the Arctic Ocean. Geophys. Res. Lett. 35, L03402. https://doi.org/10.1029/2007GL032837.

Holmes, R.M., Coe, M.T., Fiske, G.J., Gurtovaya, T., McClelland, J.W., Shiklomanov, A.I., et al., 2013. Climate change impacts on the hydrology and biogeochemistry of Arctic rivers. Clim. Change Glob. Warm. Inland Waters 1–26. https://doi.org/10.1002/9781118470596.ch1.

in't Zandt, M.H., Liebner, S., Welte, C.U., 2020. Roles of Thermokarst Lakes in a Warming World. Trends Microbiol. 28, 769–779. https://doi.org/10.1016/j.tim.2020.04.002.

Jasechko, S., Gibson, J.J., Birks, S.J., Yi, Y., 2012. Quantifying saline groundwater seepage to surface water in the Athabasca oil sands region. Appl. Geochem. 10 (10), 2068–2076.

Jiang, R., Gan, T.Y., Xie, J., Wang, N., Kao, C.-C., 2017. Historical and potential changes of precipitation and temperature of Alberta subjected to climate change impact: 1900–2100. Theor. Appl. Clim. 127, 725–739. https://doi.org/10.1007/s00704-015-1664-y.

Kelly, E.N., Short, J.W., Schindler, D.W., Hodson, P.V., Ma, M.S., Kwan, A.K., Fortin, B.L., 2009. Oil sands development contributes polycyclic aromatic compounds to the Athabasca River and its tributaries. Proc. Natl. Acad. Sci. U. S. A. 106, 22346–22351.

Kelly, E.N., Schindler, D.W., Hodson, P.V., Short, J.W., Radmanovich, R., Nielsen, C.C., et al., 2010. Oil sands development contributes elements toxic at low concentrations to the Athabasca River and its tributaries. Proc. Natl. Acad. Sci. USA 107, 16178–16183.

Kuhn, M.A., Thompson, L.M., Winder, J.C., Braga, L.P.P., Tanentzap, A.J., Bastviken, D., Olefeldt, D., 2021. Opposing effects of climate and permafrost thaw on CH_4 and CO_2 emissions from northern lakes. AGU Adv. 2, e2021AV000515. https://doi.org/10.1029/2021AV000515.

Kurek, J., Kirk, J.L., Muir, D.C.G., Wang, X., Evans, M.S., Smol, J.P., 2013. Legacy of a half century of Athabasca oil sands development recorded by lake ecosystems. Proc. Natl. Acad. Sci. 110, 1761–1766.

Li, J., Siegel, D.I., Lautz, L.K., Mitchell, M.J., Dahms, D.E., Mayer, B., 2010. Calcite precipitation driven by the common ion effect during groundwater–surface-water mixing: A potentially common process in streams with geologic settings containing gypsum. GSA Bull. 122, 1027–1038. https://doi.org/10.1130/B30011.1.

Makar, P.A., Akingunola, A., Cole, A.S., Aklilu, Y., Zhang, J., Wong, I., Hayden, K., Li, S., Kirk, J., Scott, K., Moran, M.D., Robichaud, A., Cathcart, H., Baratzedah, P., Pabla, B., Cheung, P., Zheng, Q., Jefffries, D.S., 2018. Estimates of exceedances of critical loads for acidifying deposition in Alberta and Saskatchewan. Atmos. Chem. Phys. 18, 9897–9927.

Nydahl, A.C., Wallin, M.B., Weyhenmeyer, G.A., 2020. Diverse drivers of long-term pCO2 increases across thirteen boreal lakes and streams. Inland Waters 10, 360–372. https://doi.org/10.1080/20442041.2020.1740549.

Parkhurst, D.L., Appelo, C.A.J., 1999. Description of Input and Examples for PHREEQC.Version 3.5.0.14000. A Computer Program for Speciation, Batch-Reaction, One-Dimensional Transport, and Inverse Geochemical Calculations..

Peters, D.L., Watt, D., Devito, K., Monk, W.A., Shrestha, R.R., Baird, D.J., 2022. Changes in geographical runoff generation in regions affected by climate and resource development: a case study of the Athabasca River. J. Hydrol.: Reg. Stud. 39, 100981. https://doi.org/10.1016/j.ejrh.2021.100981.

Prepas, E.E., Planas, D., Gibson, J.J., Vitt, D.H., Prowse, T.D., Dinsmore, W.P., Halsey, L.A., McEachern, P.M., Paquet, S., Scrimgeour, G.J., Tonn, W.M., Paszkowski, C. A., Wolfstein, K., 2001. Landscape variables influencing nutrients and phytoplankton communities in boreal plain lakes of northern Alberta: a comparison of wetland- and upland-dominated catchments. Can. J. Fish. Aquat. Sci. 58, 1286–1299.

RAMP (Regional Aquatics Monitoring Program), 2005. Regional Aquatics Monitoring Program 2005. Standard Operating Procedures. Hatfield Consultants. West Vancouver, BC. 78pp. http://www.ramp-alberta.org/.

Salmi, T., Määttä, A., Anttila, P., Ruoho-Airola, T., Amnell, T., 2002., Detecting trends of annual values of atmospheric pollutants by the Mann-Kendall test and Sen's slope estimates –the Excel template application MAKESENS. Publications on Air Quality No. 31, Report code FMI-AQ-31, Finnish Meteorological Institute, Air Quality Research, ISBN 951-697-563-1, 35 pp.

Saltzman, M.R., Thomas, E., 2012. Carbon isotope stratigraphy. In: Gradstein, F.M., Ogg, J.G., Schmitz, M., Ogg, G. (Eds.), Geol. Time Scale 207–232. https://doi.org/10.1016/B978-0-444-59425-9.00011-1.

Schindler, D.W., 2014. Unravelling the complexity of pollution by the oil sands industry. PNAS 111, 3209–3210.

Schmidt, A., Gibson, J.J., Santos, I.R., Shubert, M., Tattrie, K., Weiss, H., 2010. The contribution of groundwater discharge to the overall water budget of lakes in Alberta/Canada estimated from a radon mass balance. Hydrol. Earth Syst. Sci. 14, 79-89.

Schuur, E.A.G., McGuire, A.D., Romanovsky, V., Schädel, C., Mack, M., 2018. Chapter 11: Arctic and boreal carbon. In: Cavallaro, N., Shrestha, G., Birdsey, R., Mayes, M.A., Najjar, R.G., Reed, S.C., Romero-Lankao, P., Zhu, Z. (Eds.), In Second State of the Carbon Cycle Report (SOCCR2): A Sustained Assessment Report. U. S. Global Change Research Program, Washington, DC, USA. https://doi.org/10.7930/SOCCR2.2018.Ch11.

Schuur, E.A.G., Abbott, B.W., Commane, R., Ernakovich, J., Euskirchen, E., Hugelius, G., et al., 2022. Permafrost and climate change: Carbon cycle feedbacks from the warming arctic. Annu. Rev. Environ. Resour. 47, 343–371. https://doi.org/10.1146/annurev-environ-012220-011847.

Smerdon, B.D., Devito, K.J.U., Mendoza, C.A., 2005. Interaction of groundwater and shallow lakes on outwash sediments in the sub-humid Boreal Plains of Canada. J. Hydrol. 314, 246–262.

Spence, C., Woo, M.K., 2003. Hydrology of subarctic Canadian Shield: Soil-filled valleys. J. Hydrol. 279, 151–166. https://doi.org/10.1016/s0022-1694(03)00175-6.

Spence, C., Norris, M., Bickerton, G., Bonsal, B.R., Brua, R., Culp, J.M., Dibike, Y., Gruber, S., Morse, P.D., Peters, D.L., Shrestha, R., Wolfe, S.A., 2020. The Canadian water resource vulnerability index to permafrost thaw (CWRVIPT). Arct. Sci. 6, 437–462. https://doi.org/10.1139/as-2019-0028.

Summers, J.C., Kurek, J., Kirk, J.L., Muir, D.C.G., Wang, X., Wiklund, J.A., Cooke, C.A., Evans, M.S., J.P., 2016. Recent warming, rather than industrial emissions of bioavailable nutrients, is the dominant driver of lake primary production shifts across the Athabasca oil sands region. PLoS ONE 11, e0153987.

Tattrie, K., 2011. Groundw. Surf. Water Interact. a Wetl. Rich., Low. Relief Boreal Environ. M. Sc. Thesis, Univ. Vic. 21.

Vitt, D.H., Halsey, L.A., Zoltai, S.C., 1994. The bog landforms of continental western Canada in relation to climate and permafrost patterns. Arct. Alp. Res. 26, 1–13.

Vitt, D.H., Halsey, L.A., Zoltai, S.C., 2000. The changing landscape of Canada's western boreal forest. Can. J. For. Res. 30, 283–287. https://doi.org/10.1139/x99-214.

Vitt, D.H., House, M., Glaeser, L., 2022. The response of vegetation to chemical and hydrological gradients at a patterned rich fen in northern Alberta, Canada. J. Hydrol.: Reg. Stud. 40, 101038. https://doi.org/10.1016/j.ejrh.2022.101038.

Walvoord, M.A., Streigl, R.G., 2021. Complex Vulnerabilities of the Water and Aquatic Carbon Cycles to Permafrost Thaw. Front. Clim. 3, 730402. https://doi.org/10.3389/fclim.2021.730402.

Wan, C., Li, K., Shen, S., Gibson, J.J., Ji, K., Yi, P., Yu, Z., 2019b. Using tritium and ^{222}Rn to estimate groundwater discharge and thawing permafrost contributing to surface water in permafrost regions on Qinghai – Tibet Plateau. J. Radioanal. Nucl. Chem. 322, 561–578. https://doi.org/10.1007/s10967-019-06720-5.

Wan, C., Gibson, J.J., Shen, S., Yi, P., Yu, Z., 2019a. Using stable isotopes paired with tritium analysis to assess thermokarst lake water balances in the Source Area of the Yellow River, northeastern Qinghai-Tibet Plateau, China. Sci. Total Environ. 689, 1276–1292. https://doi.org/10.1016/j.scitotenv.2019.06.427.

Wan, C., Gibson, J.J., Peters, D.L., 2020. Isotopic constraints on water balance of tundra lakes and watersheds disturbed by permafrost degradation in the Mackenzie Delta region, Northwest Territories, Canada. Sci. Total Environ. 731, 139176. https://doi.org/10.1016/j.scitotenv.2020.139176.

Webb, E.E., Liljedahl, A.K., Cordeiro, J.A., et al., 2022. Permafrost thaw drives surface water decline across lake-rich regions of the Arctic. Nat. Clim. Chang. 12, 841–846. https://doi.org/10.1038/s41558-022-01455-w.

Whitfield, C.J., Aherne, J., Gibson, J.J., Seabert, T.A., Watmough, S.A., 2010. The spatial and temporal geochemical analysis of three boreal peatland complexes. Hydrol. Process. 24, 2143–2155. https://doi.org/10.1002/hyp.7637.

WRS (Western Resource Solutions), 2006. Critical Loads of Acidity to Lakes in the Athabasca Oil Sands Region - Modification of the Henriksen Model for Lake Organic Content. Final report to: NOx-SOx Management Working Group, Fort McMurray, Alberta. January, 2006.

Wu, X., Macdonald, R., Wu, T., 2023. Coupled changes in the Arctic carbon cycle between the land, marine, and social domains. Earth'S. Future 11, e2022EF003293. https://doi.org/10.1029/2022EF003293.

Zabel, N.A., Soliguin, A.M., Wiklund, J.A., Birks, S.J., Gibson, J.J., Fan, X., Wolfe, B.B., Hall, R.I., 2021. Paleolimnological assessment of past hydro-ecological variation at a shallow hardwater lake in the Athabasca Oil Sands Region before potential onset of industrial development. J. Hydrol. Reg. Stud. 39, 100977. https://doi.org/10.1016/j.ejrh.2021.100977.

Zolkos, S., Tank, S.E., 2020. Experimental evidence that permafrost thaw history and mineral composition shape abiotic carbon cycling in thermokarst-affected stream networks. Front. Earth Sci. 8, 152. https://doi.org/10.3389/feart.2020.00152.